Cell Reports

Report

ADA2 is a lysosomal deoxyadenosine deaminase acting on DNA involved in regulating TLR9-mediated immune sensing of DNA

Graphical abstract

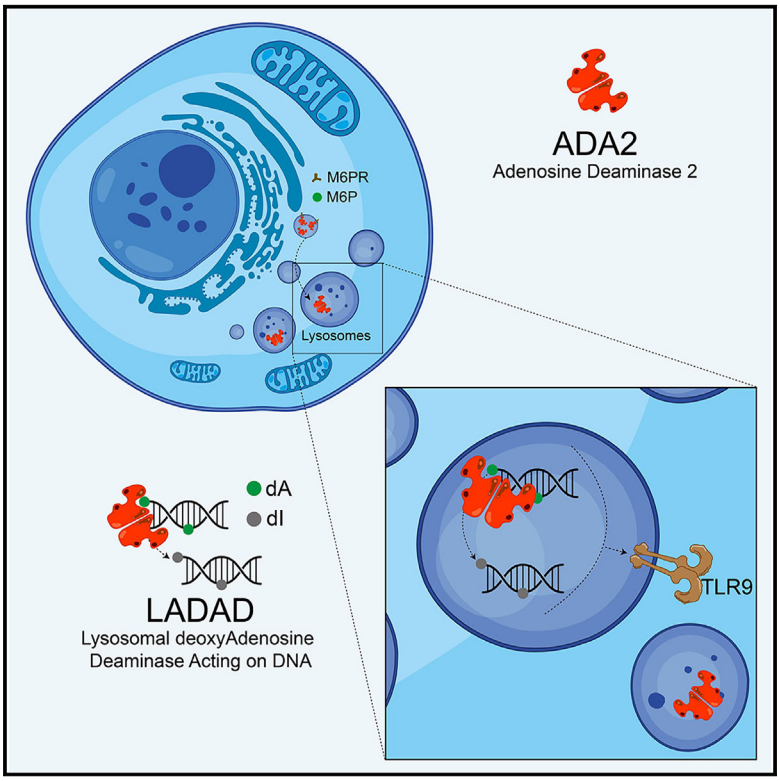

Authors

Ole Kristian Greiner-Tollersrud, Máté Krausz, Vincent Boehler, ..., Ingrun Alseth, Max Warncke, Michele Proietti

Correspondence

michele.proietti@uniklinik-freiburg.de

In brief

Greiner-Tollersrud et al. discover ADA2's function as a lysosomal deoxyadenosine deaminase acting on DNA (LADAD). This finding reveals insights into cellular DNA sensing and innate immune regulation, with potential implications for therapeutic approaches and gene editing applications.

Highlights

- ADA2 is primarily a lysosomal protein, challenging the notion of its predominant extracellular presence
- ADA2 is capable of editing DNA by converting deoxyadenosine to deoxyinosine
- Lysosomal ADA2's DNA editing activity modulates DNA sensing and innate immune responses

Greiner-Tollersrud et al., 2024, Cell Reports *43*, 114899
November 26, 2024
https://doi.org/10.1016/j.celrep.2024.114899

CellPress

Cell Reports

CellPress
OPEN ACCESS

Report

ADA2 is a lysosomal deoxyadenosine deaminase acting on DNA involved in regulating TLR9-mediated immune sensing of DNA

Ole Kristian Greiner-Tollersrud,[1,23] Máté Krausz,[2,23] Vincent Boehler,[3] Aikaterini Polyzou,[4,5] Maximilian Seidl,[6] Ambra Spahiu,[2] Zeinab Abdullah,[7] Katarzyna Andryka-Cegielski,[8] Felix Immunuel Dominick,[8] Katrin Huebscher,[2,9] Andreas Goschin,[2] Cristian R. Smulski,[10] Eirini Trompouki,[4,5] Regina Link,[3] Hilmar Ebersbach,[3,22] Honnappa Srinivas,[3] Martine Marchant,[3] Georgios Sogkas,[11,12] Dieter Staab,[3] Cathrine Vågbø,[13] Danilo Guerini,[3] Sebastian Baasch,[2,14,15] Eicke Latz,[16] Gunther Hartmann,[8] Philippe Henneke,[2,14] Roger Geiger,[17,18] Xiao P. Peng,[19] Bodo Grimbacher,[2,20] Eva Bartok,[8,23] Ingrun Alseth,[21,23] Max Warncke,[3,23] and Michele Proietti[2,11,12,23,24,*]

[1]Institute of Medical Biology, University of Tromsø, Tromsø, Norway
[2]Institute for Immunodeficiency, Center for Chronic Immunodeficiency, Medical Center, Faculty of Medicine, Albert-Ludwigs-University of Freiburg, Freiburg im Breisgau, Germany
[3]Novartis Institutes for Biomedical Research, 4056 Basel, Switzerland
[4]Max Planck Institute of Immunobiology and Epigenetics, Freiburg, Germany
[5]IRCAN Institute for Research on Cancer and Aging, INSERM Unité 1081, CNRS UMR 7284, Université Côte d'Azur, Nice, France
[6]Institute of Pathology, University Hospital of Düsseldorf, Düsseldorf, Germany
[7]Institute of Experimental Immunology, Universitätsklinikum Bonn, Bonn, Germany
[8]Institute of Experimental Hematology and Transfusion Medicine Bonn, Bonn, Germany
[9]Institut für Forstentomologie und Waldschutz, Albert-Ludwigs-University of Freiburg, Freiburg im Breisgau, Germany
[10]Medical Physics Department, Centro Atómico Bariloche, Comisión Nacional de Energía Atómica (CNEA), Consejo Nacional de Investigaciones Científicas y Técnicas (CONICET), San Carlos de Bariloche, Río Negro, Argentina
[11]Department of Rheumatology and Clinical Immunology, Hannover Medical School, Carl-Neuberg-Str. 1, 30625 Hannover, Germany
[12]RESIST - Cluster of Excellence 2155, Hannover Medical School, Carl-Neuberg-Str. 1, 30625 Hannover, Germany
[13]Proteomics and Modomics Experimental Core (PROMEC), Norwegian University of Science and Technology and the Central Norway Regional Health Authority, Trondheim, Norway
[14]Institute for Infection Prevention and Control, Medical Center - University of Freiburg, Faculty of Medicine, University of Freiburg, Freiburg, Germany
[15]Freiburg Institute for Advanced Studies (FRIAS), University of Freiburg, Freiburg, Germany
[16]Institute of Innate Immunity, Universitätsklinikum Bonn, Bonn, Germany
[17]Institute for Research in Biomedicine, Università della Svizzera italiana, Bellinzona, Switzerland
[18]Institute of Oncology Research, Università della Svizzera italiana, Bellinzona, Switzerland
[19]Department of Genetic Medicine, Johns Hopkins University School of Medicine, Baltimore, MD, USA
[20]RESIST - Cluster of Excellence 2155 to Hanover Medical School, Satellite Center Freiburg, Freiburg, Germany
[21]Department of Microbiology, Oslo University Hospital, Oslo, Norway
[22]Present address: ImmunOs Therapeutics, Schlieren, Switzerland
[23]These authors contributed equally
[24]Lead contact
*Correspondence: michele.proietti@uniklinik-freiburg.de
https://doi.org/10.1016/j.celrep.2024.114899

SUMMARY

Although adenosine deaminase 2 (ADA2) is considered an extracellular ADA, evidence questions the physiological relevance of this activity. Our study reveals that ADA2 localizes within the lysosomes, where it is targeted through modifications of its glycan structures. We show that ADA2 interacts with DNA molecules, altering their sequences by converting deoxyadenosine (dA) to deoxyinosine (dI). We characterize its DNA substrate preferences and provide data suggesting that DNA, rather than free adenosine, is its natural substrate. Finally, we demonstrate that dA-to-dI editing of DNA molecules and ADA2 regulate lysosomal immune sensing of nucleic acids (NAs) by modulating Toll-like receptor 9 (TLR9) activation. Our results describe a mechanism involved in the complex interplay between NA metabolism and immune response, possibly impacting ADA2 deficiency (DADA2) and other diseases involving this pathway, including autoimmune diseases, cancer, or infectious diseases.

INTRODUCTION

Humans possess two adenosine deaminases (ADAs), named ADA1 and ADA2. ADA2 differs from ADA1 in several aspects, including molecular mass, the existence of a homodimer instead of a monomer, different optimum pH, and insensitivity to inhibition by EHNA (eritron-9-2-hydroxy-3-nonyl-adenine).[1–3] In addition, unlike ADA1, ADA2 is considered to function predominantly in the extracellular space.[3–5] Some measurements, however, indicate that at physiological concentrations of Ado, the extracellular activity of ADA1 far exceeds that of ADA2.[6] This, coupled with the fact that ADA2 has approximately 100-fold lower affinity than ADA1 for free adenosine (Ado), casts doubt on the biological relevance of ADA2-mediated extracellular Ado deamination. Of consequence, what the true function of ADA2 is and why its absence leads to self-inflammation[7–11] remain highly debated.

Nucleic acid sensing (NAS) is a basic mechanism of immune activation.[12] It is crucial for antiviral defense in vertebrates, but its dysfunctions cause autoinflammatory or autoimmune diseases.[13]

Here, we discovered that ADA2 is a lysosomal protein that binds DNA and efficiently deaminates deoxyadenosine (dA) residues of DNA to deoxyinosine (dI), suggesting that DNA is its natural substrate. We also found that dA-to-dI editing of DNA and ADA2 facilitates immune detection of DNA mediated by Toll-like receptor 9 (TLR9).

By elucidating ADA2's role in DNA sensing and metabolism, this study expands our understanding of innate immunity and sheds light on potential therapeutic targets for autoimmune and autoinflammatory diseases.

RESULTS

ADA2 is a lysosomal protein

In blood, ADA2 is expressed preferentially in monocytes (https://www.proteinatlas.org/ENSG00000093072-ADA2/immune+cell; Figures S1A–S1C). To obtain data on ADA2 expression in macrophages, we analyzed human tonsils (proteinatlas-CD68-tonsil). We found that ADA2 was almost exclusively expressed by tingible body macrophages (TBMs) in the germinal center (Figures 1A and 1B), with few dendritic cells (DCs) in the crypt epithelium and surface epithelium containing ADA2-positive intracytoplasmic granules (Figures 1A and 1B). More interestingly, at higher magnification, the ADA2-derived signal resembled phagolysosomes (Figure 1C). We tested whether ADA2 localizes in lysosomes, by immunofluorescence, co-staining ADA2 and LAMP1, a glycoprotein expressed in lysosomes and late endosomes. These experiments revealed that ADA2 is contained in LAMP1-positive lysosomes (Figures 1D–1F and S1D). We confirmed ADA2 to be a lysosomal protein in peripheral monocytes, plasmacytoid DCs (pDCs), and conventional DCs (cDCs) (Figures 1G–1I and S1F). The specificity of the ADA2 signal was assessed using monocytes from patients with ADA2-deficiency (DADA2) (Figures 1J and 1K) and performing fluorescence minus one (FMO) controls (Figure S1E).

To reach the lysosome, soluble proteins are tagged with mannose-6-phosphate (M6P),[15] which is recognized by the M6P receptor. In 2006, Sleat et al.[16] purified M6P glycoproteins from human plasma and hypothesized that ADA2 was a lysosomal protein. This result suggests that ADA2 could be targeted to endolysosomes via the M6P-dependent pathway. ADA2 orthologs (Figures S1G and S1H) are present in all mammals except rodents. Furthermore, the protein is highly expressed in microglia (Figure S1I). Thus, we purified endogenous ADA2 from porcine brain to access sufficient material for glycan analysis. We found that porcine ADA2 (pA2) contains a significant amount of M6P-modified glycans linked to three of its glycosylation sites (N127, N174, N378) (Figure 1L). In addition, its glycan profile echoes those of known lysosomal proteins, such as lysosomal alpha-mannosidase (LAMAN), phospholipase D3 (PLD3), and ependymin-related protein 1 (EPDR1), and it is distinct from those of extracellular proteins such as oligodendrocyte myelin glycoprotein (OMgp) and signal regulatory protein alpha (SIRPα) (Figure 1L). These results indicate that ADA2 is a lysosomal protein targeted to endolysosomes via the M6P-dependent pathway.

ADA2 interacts with DNA

The discovery of its lysosomal localization and the fact that its ADA activity on free Ado is further reduced by a pH below six[1,17] encouraged us to investigate whether ADA2 has an alternative function. Both ADA1 and ADA2 accommodate a purine in the active site pocket. However, ADA2 possesses an enlarged pocket that may adapt the purine-linked ribose units of large nucleotide-containing molecules, such as DNA or RNA.[18] We also observed that in contrast to ADA1 (Figure 2A), the area surrounding the active site of ADA2 is positively charged (Figure 2B), which could facilitate interactions with negatively charged molecules such as NAs.

We modeled the binding of ADA2 with a double-stranded DNA (dsDNA) molecule by using HDOCK,[19] and the top-scoring model suggested an interaction between dsDNA and the PRB domain of ADA2 (Figure 2C), which is absent in ADA1 (Figures 2A, 2B, and S2A). The residues predicted to be involved are two lysine residues flanking cysteine 133, which forms a disulfide bridge with cysteine 111 (Figures S2B and S2C).

Having insight into the protein's ability to bind DNA, we wanted to confirm this experimentally. We first produced the human recombinant (hr)ADA2 (Figures S2D–S2G). The fluorescence resonance energy transfer (FRET) assay can assess the interaction between DNA and proteins.[20] As shown in Figure 2D and 2E, hrADA2, but not ADA1, induced a significant FRET signal with an optimal pH = 5, resembling a lysosomal environment. The ADA2-mediated FRET signal was induced without degradation of the oligos, indicating that the signal is caused only by ADA2-DNA interactions (Figure S3A).

We further evaluated ADA2's interaction with DNA and the specific structural preferences it may have using an electrophoretic mobility shift assay (EMSA). This assay confirmed that ADA2 binds to different DNA substrates (Figures 2F and 2G; Table S1), including single-stranded DNA (ssDNA) and complex/branched DNA molecules (Hairpin [HpTT], Pseudo-Y, and 5′Flap-DNA). The strongest shifts were obtained with substrates containing regions of both dsDNA and ssDNA (Hairpin and Pseudo-Y). We also found that ADA2 shows a higher binding affinity for longer DNA substrates (Figure 2H; HpTT42 to HpTT20).

CellPress
OPEN ACCESS

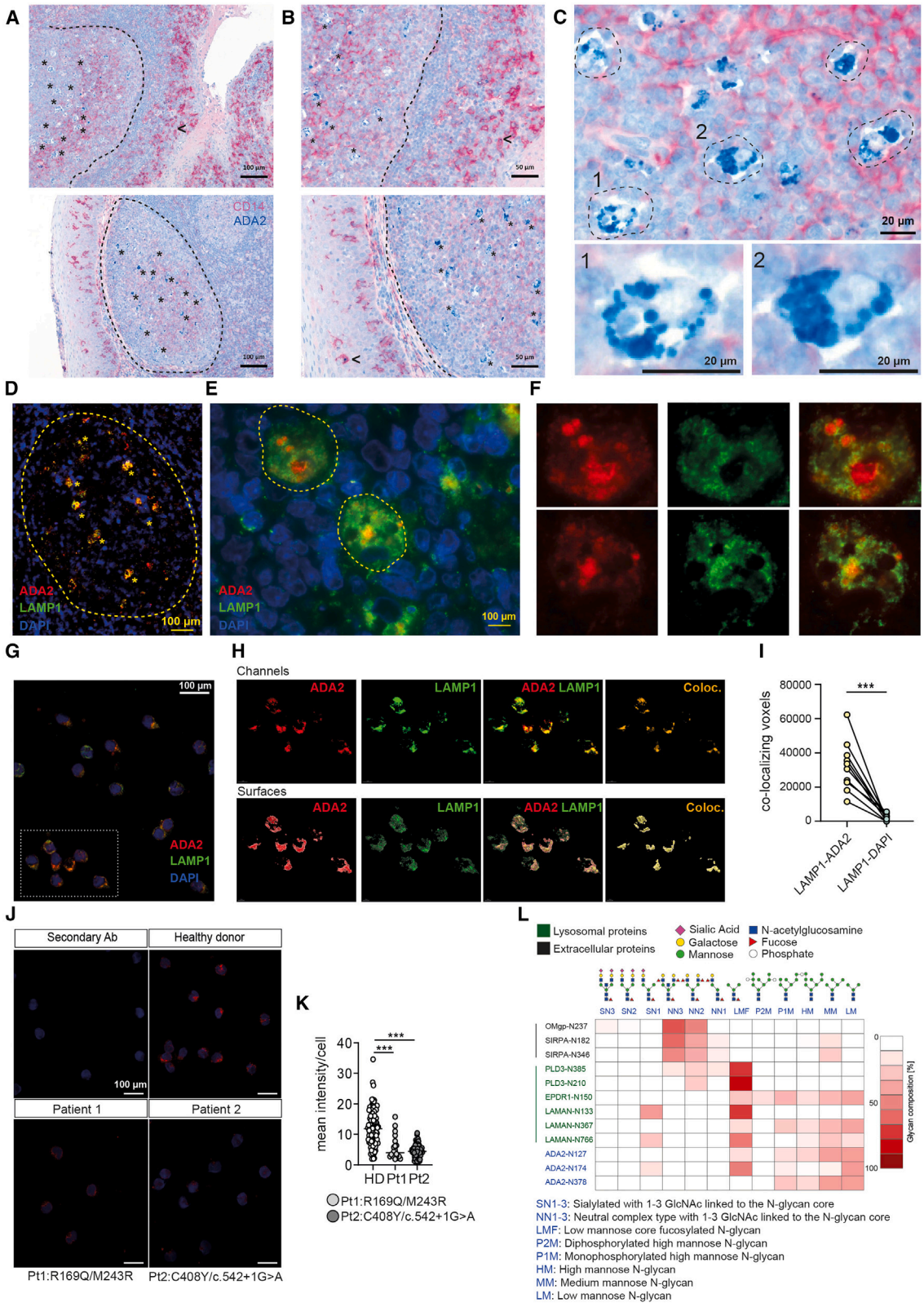

(legend on next page)

Moreover, increasing the pH from 5.5 to 7.5 decreased, but did not abolish, ADA2-DNA binding (Figures 2I and 2J). Finally, evaluating several ADA2 mutant proteins (Table S2) revealed a positive correlation between ADA2 deaminase activity on free Ado and the FRET signal (Figures 2K, S3B, and S3C). Similarly, ADA2 mutant proteins with different ADA activity showed different DNA-binding affinities (Figure 2L). These results suggested that the change in DNA conformation might relate to the ADA catalytic activity or catalytic site of ADA2, one of the hypotheses being the conversion of the dA nucleobase to dI, as suggested further by the inhibition mediated by deoxycoformycin, a potent inhibitor of ADA2-mediated ADA activity[18] (Figures S3D and S3E).

ADA2 is a lysosomal dA deaminase acting on DNA

To examine if ADA2 deaminates dA on DNA, we performed the *Escherichia coli* endonuclease V (EcEndoV) assay (Figures 3A and S4A). Incubation of DNA substrates (Figure 3B; Table S1) with ADA2 led to the emergence of cleavage products after EcEndoV treatment, with optimal activity at pH 5.5 (Figures 3C and 3D). Dot blot analysis using an anti-inosine antibody (Figure S4B) was also consistent with ADA2-mediated dA-to-dI activity (Figure 3E) and the quantification of dI residues through mass spectrometry (Figure 3F; Table S3). The signal observed on the dot blot and the measured dIs were higher for oligonucleotides (ODNs) with terminal dAs. Cleavage of an ODN with a 5′ dI by EcEndoV will generate a 2-nt fragment (Figure S4A). Separating the ADA2-EcEndoV sample by DNA sequencing gel electrophoresis gave a 2-nt product (Figure 3G), confirming that ADA2 deaminates preferentially terminal 5′ and 3′ dA residues. Lysosomal DNA is likely processed by lysosomal endonucleases that can generate nicks or DNA double-strand breaks and, therefore, additional terminal ends. We thus tested whether the protein could perform dA-to-dI activity on nicked DNA terminals by comparing different ODNs, as shown in Figure S4C. These experiments confirmed that the protein can deaminate dA residues on nicked terminals of DNA (Figure S4C).

ADA2-mediated dA-to-dI activity could be detected with a meager amount of ADA2 (<1 nM), indicating that ADA2 has a higher affinity toward DNA-dA than free Ado, suggesting that DNA is its natural substrate. In agreement, the dA-to-dI editing activity could be inhibited by equimolar amounts of "cold" DNA but not by a 10,000-fold excess of free Ado or free dA (Figure 3H). Competition of the cold DNA on the EcEndoV activity was excluded by assessing the effect of increasing amounts of unlabeled DNAs on the cleavage of an end-labeled ODN containing dI by EcEndoV (Figure S4D). ADA2-mediated adenosine-to-inosine (A-to-I) activity toward RNA was also observed, albeit at lower efficiency than toward DNA (Figure S4E). We finally tested if the catalytic site of ADA2 mediates the dA-to-dI activity. For this, we compared mutant ADA2 proteins with different ADA activity (Figure 2K). dA-to-dI activity was absent in the catalytic dead mutant G358R, demonstrating that the catalytic site of ADA2 indeed mediates dA-to-dI activity (Figure 3I), as further confirmed by the inhibition mediated by deoxycoformycin (Figure 3H).[18] Finally, dA-to-dI editing activity was also shown by endogenous pA2 (Figure 3G). Importantly, ADA1 did not perform dA-to-dI deamination (Figures 3J, 3K, and S4F).

dA deamination of DNA molecules and ADA2 control lysosomal DNA sensing, facilitating TLR9 activation

Given its lysosomal localization and the ability to bind and edit DNA, we hypothesized that ADA2 may regulate lysosomal DNA sensing. Lysosomal DNA sensing is mediated by TLR9, which recognizes unmethylated CpG motifs in ssDNA.[12,21–24] Whether dI is recognized by TLR9 is currently not known. However, dI in DNA is generally recognized as deoxyguanosine (dG) by cellular proteins.[25] Thus, we investigated whether dI residues in DNA molecules could be "recognized as" dG by TLR9. We modified the human CpG2216 (A-class CpG) TLR9 ligand[26] by replacing the dG residues known to be essential for TLR9 activation with dI (named CpI) or cytosine (CpC) (Figure 4A). These ODNs were tested in human-TLR9 HEK-Blue reporter cells (Figure 4B). CpI showed similar activity to CpG (Figure 4B), indicating that TLR9 can recognize dI. Analogous results were obtained for type I interferon (IFN) production in human peripheral blood mononuclear cells (PBMCs) (Figure 4C). Additional experiments using ODNs where dA residues have been substituted by dI residues (Figure 4D) confirmed that dA-to-dI editing of DNA molecules shapes the potency of possible TLR9 ligands (Figure 4E).

Figure 1. ADA2 is a lysosomal protein

(A and B) CD14 (red) and ADA2 (blue) staining of a human tonsil. (A) Germinal centers (black dotted line) with cytoplasmic ADA2 positivity in tingible body macrophages (TBMs) (marked by asterisks in the top and bottom images), whereas CD14 highlights the follicular dendritic cell meshwork (10× original magnification). In higher magnifications (B), $CD14^+$ dendritic cells[14] in the crypt epithelium (top) and surface epithelium (bottom) show few small ADA2-positive intracytoplasmic granules (highlighted by arrowheads, exemplary; 20× original magnification).

(C) Higher magnification (40× original magnification) showing TBMs (black dotted line) containing ADA2-positive organelles resembling phagolysosomes. Two TBMs are further magnified in the bottom images.

(D) Immunofluorescence of human tonsils showing ADA2-positive cells (yellow asterisks) in the germinal centers (yellow dotted line) (20× original magnification).

(E) Higher (40×) magnification of TBMs with LAMP1-positive lysosomes containing ADA2.

(F) Color channels from the images in (E) show single staining of ADA2 (red) and LAMP1 (green).

(G) Expression of ADA2 (red) and LAMP1 (green) in monocytes.

(H) Color channels (top row) and surface channels (bottom row) rendered with Imaris show the signals of ADA2 and LAMP1. The right image shows the co-localization signal rendered by Imaris.

(I) Quantification of co-localization expressed as co-localizing voxels. Co-localization between nuclear (DAPI) and ADA2 has been measured as negative control (***$p < 0.0001$, Mann-Whitney test).

(J) Expression of ADA2 in monocytes from healthy donors and two DADA2 patients.

(K) Quantification of ADA2 expression from the images in (J) expressed as mean intensity per cell (**$p < 0.001$ and ***$p < 0.0001$, Kruskal-Wallis test).

(L) Heatmap comparing the glycan structures of pA2 and other lysosomal (green) and extracellular (black) proteins. The color scale represents the percentage of glycans linked to the indicated amino acid residues.

CellPress
OPEN ACCESS

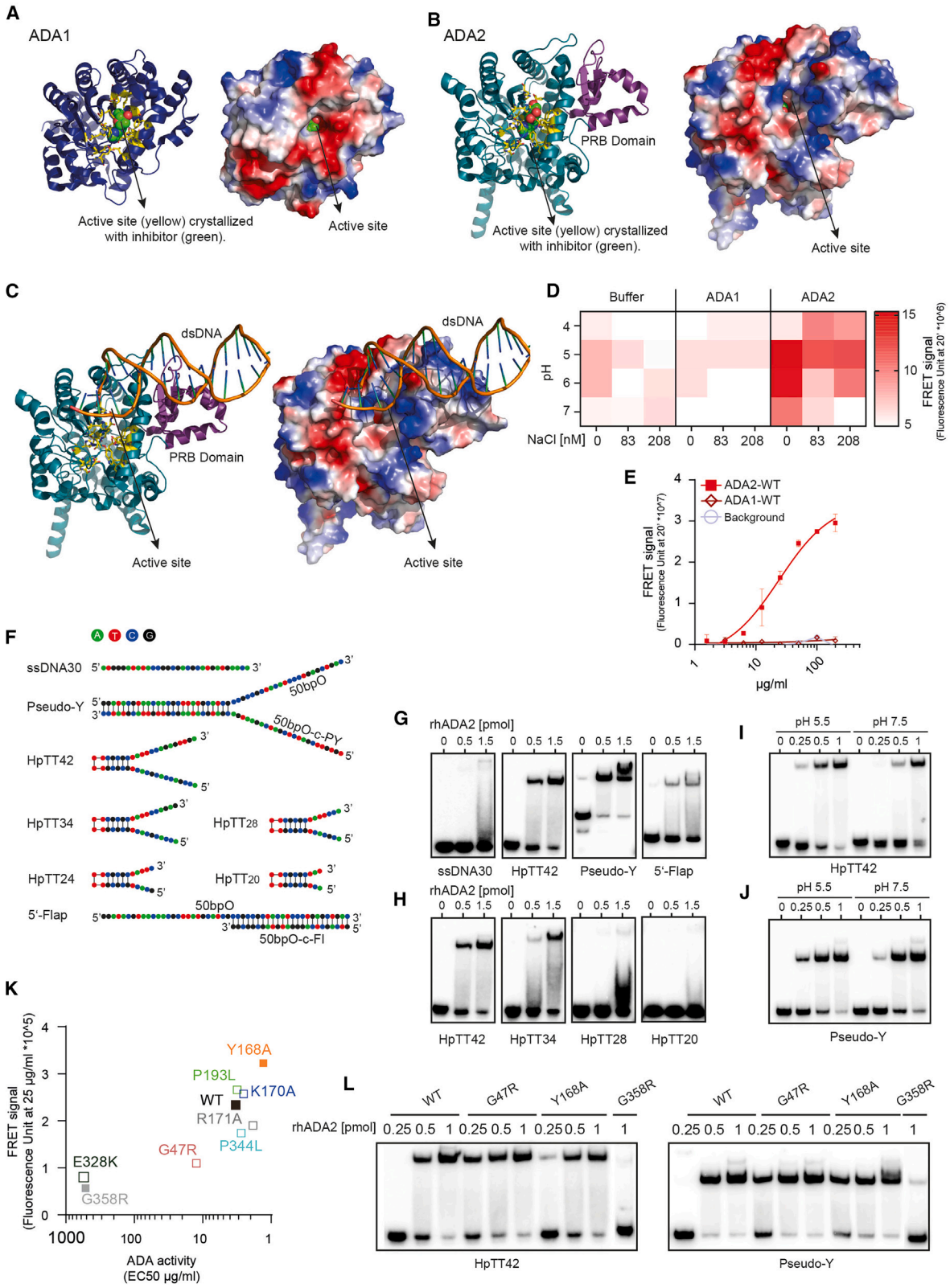

(legend on next page)

We then transduced the HEK-human TLR9 reporter cells with lentiviruses encoding ADA2-GFP or GFP only. We found ADA2 expression to be associated with the significant upregulation of TLR9 signaling upon CpG2216 stimulation (Figure S5A). We used additional HEK293T reporter cell lines with stable TLR7 or TLR9 expression and molecular chaperone UNC93B1 expression to confirm this finding.[27] These cells secreted interleukin (IL)-8 upon activation of the respective receptor and were stimulated with CpG2006 (B-class CpG),[28] CpG2216, R848 (TLR7/8 small-molecule agonist), and dsDNA from *E. coli*. ADA2 significantly increases TLR9 activation upon stimulation with CpG2216 and *E. coli* DNA, while no differences were observed upon stimulation with CpG2006 and R848 (Figures 4F and S5B). We then tested PBMCs from DADA2 patients and healthy controls. IFN-α was used as a readout for TLR9 activation in pDCs,[29] while tumor necrosis factor alpha (TNF-α) was used as a readout for CpG2006. The TLR7/8 stimulus 9.2s RNA[30] was included to control for the activity of DCs in DADA2 patients since a reduction in their number could have also led to a reduced TLR9 response. We observed a significant decrease of IFN-α production in cells from DADA2 patients upon CpG2216 stimulation but not for TNF-α after CpG2006 stimulation (Figures 4G and 4H). We confirmed these results in pDCs and cDCs sorted (Figures S5C and S5D) from DADA2 patients and healthy controls (Figure 4I).

As described above, ADA2 efficiently converts Ado residues at the terminal 5′ and 3′ ends. As shown in Figure 4J, stimulation with CpG-derived ODNs where the 5′ dA was substituted with dI was associated with a significant upregulation of the type I IFN production compared to the non-edited analog.

CpG ODN is artificially modified by longer phosphorothioated backbones, which are generally not seen in naturally occurring DNA. To mimic natural TLR9 sensing, a longer (69-bp) dsDNA fragment was additionally tested. We separated different immune populations from PMBCs using fluorescence-activated cell sorting and then stimulated them with the 69-bp dsDNA using poly-L-arginine (PLA), an endolysosomal transfection reagent.[31] In this setting, dsDNA stimulation produces type I IFN selectively in DCs (Figure S5E). We found cells from DADA2 patients associated with impaired type I IFN production upon lysosomal dsDNA stimulation (Figure 4K). These results indicate that ADA2 and dA-to-dI conversion modulate lysosomal DNA sensing by enhancing TLR9 ligand activity.

DISCUSSION

We describe an intracellular role of ADA2 in lysosomes, identify DNA as its substrate, and describe a previously unknown regulatory mechanism of lysosomal DNA sensing and metabolism.

Despite ADA2 being hypothesized to be a lysosomal protein in 2006,[16] it is currently considered a secretory protein. The secretion of lysosomal proteins is a complex phenomenon relevant to many cellular functions, including immune response. The fact that monocytes can secrete ADA2[4] and that elevated levels of plasma ADA2 are found in diseases with signs of monocyte activation, such as in chronic inflammatory diseases[32–34] or infectious diseases,[35] suggests that the cellular trafficking of ADA2 must be regulated during the immune response. A better understanding of this regulation could provide insights into the role of ADA2 in the immune response and facilitate the development of a replacement therapy.

Our results indicate that ADA2, unlike ADA1, uses DNA as a substrate. The protein, therefore, could be evolved to interact with DNA and deaminate dA. ADA2 would thus belong to the family of proteins with NA editing activity, effectively expanding it. Indeed, to our knowledge, it is the only lysosomal protein with selective dA-to-dI activity naturally occurring on DNA so far described in mammals. The only proteins described as capable of dA-to-dI action on DNA to date are human ADAR and ADAT2 (BjADAT2) from *Branchiostoma japonicum*. ADAR is a cytosolic ADA that naturally recognizes RNA and can deaminate dA in DNA/RNA hybrids, in the presence of a dA-C mismatch, and with E-to-Q mutations.[36] BjADAT2, in complex with BjADAT3, can perform A-to-I editing of tRNA as well as dC-to-dU and dA-to-dI deamination of DNA.[37]

Given ADA2's selectivity for dA, our discovery could help accelerate the development of new genome editing tools based on dA-to-dI conversion.[38,39]

From an evolutionary point of view, ADA2 of *Sus scrofa* also possesses dA-to-dI deamination, suggesting that this activity is maintained across species. Evaluating the DNA activity of

Figure 2. ADA2 interacts with DNA substrates

(A and B) Comparison of the active sites of ADA1 and ADA2. Red represents acidic (negative) charges in the surface electrostatic charge distribution, whereas blue represents basic (positive) charges. Compared to ADA1, the catalytic site of ADA2 is surrounded by a positively charged area extending from the PRB domain to the catalytic site (B). In the cartoon representation, the active sites are shown in yellow, crystallized with inhibitors (2′-deoxyadenosine for ADA1 and coformycin for ADA2).

(C) Model of human ADA2 binding to dsDNA (PDB: 3LGD). The top-scored model corresponds to the interaction of the dsDNA molecule with the PRB domain. The cartoon on the left shows that the PRB domain (colored in purple) is located close to the active site (colored yellow and shown as sticks, whereas the rest of the protein is shown as a cartoon) and places the DNA at the top of the catalytic cleft. On the right, the electrostatic charge distribution of ADA2 is shown.

(D) Evaluation of the interaction between ADA2 and ADA1 and DNA as a measure of FRET at different pH or NaCl values.

(E) Evaluation of the ADA2- and ADA1-induced FRET signals at different protein concentrations and pH 5.5.

(F) Diagrams showing structures and sequences of the ODN used (O, oligonucleotide; c, complementary; PY, Pseudo-Y; Fl, Flap).

(G) ADA2 binding to DNA as measured by EMSA. hrADA2 was incubated with various [γ-^{32}P]-labeled DNA substrates at pH 5.5 before separating bound and free DNA on 7% native polyacrylamide gels.

(H–J) EMSA was performed also with [γ-^{32}P]-labeled DNA substrates of different lengths (H) or at pH 5.5 or 7.5 (I and J).

(K) Correlation between FRET signal (y axis, fluorescence measured at 575 nm) and ADA activity (x axis, EC50 in μg/mL) for the wild-type hrADA2 and ADA2 mutant proteins.

(L) Binding to DNA of hrADA2 mutant proteins tested by EMSA as in (G).

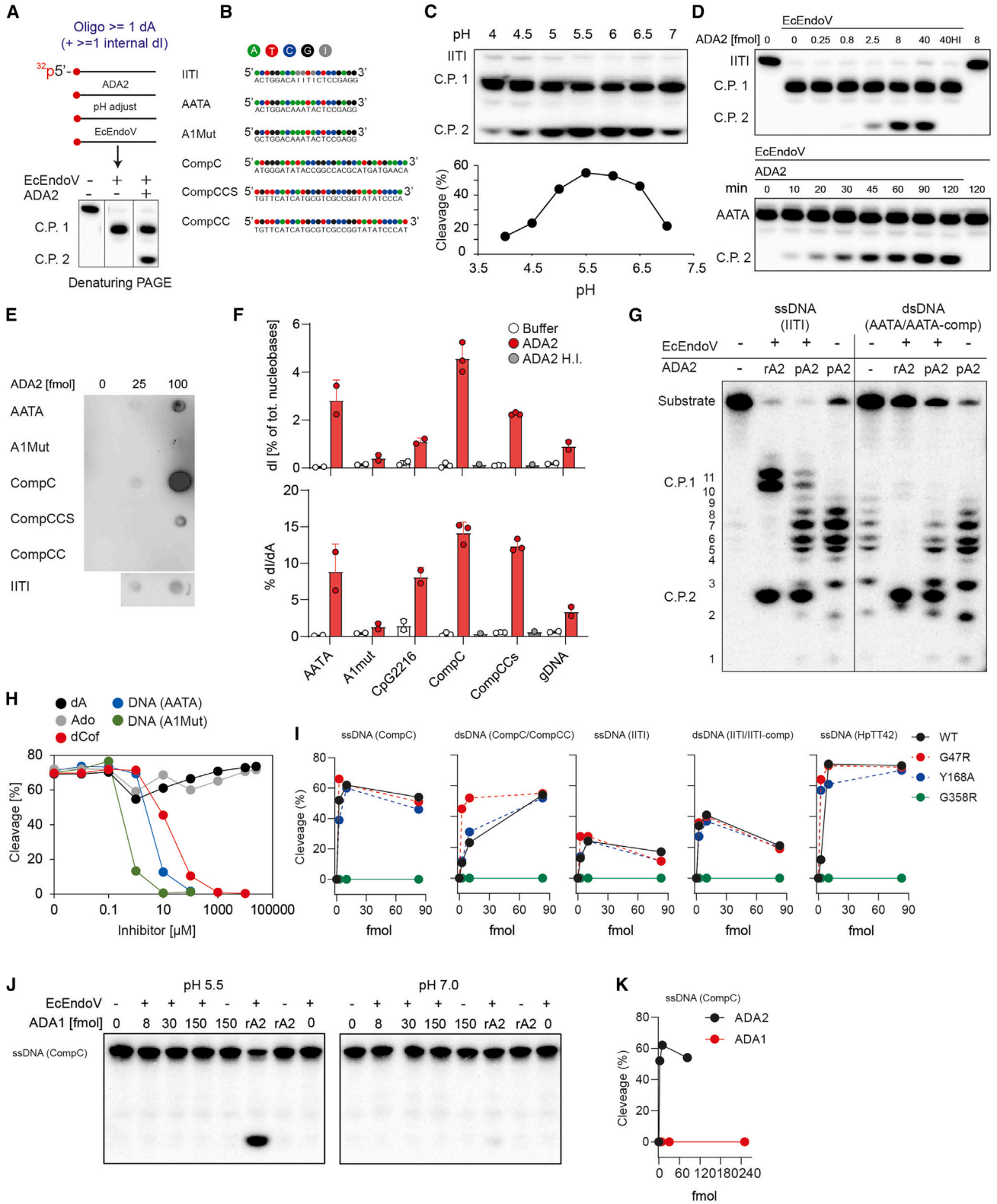

(legend on next page)

other ADA2 orthologs will help to understand why some organisms have evolved DNA-directed activity and solve the riddle of why other species, such as the mouse, despite not having ADA2, do not show a clinical phenotype superimposed on ADA2 deficiency in humans. One possibility is that an unidentified protein has ADA2-like activity on DNA.

In addition to the repercussions just described, it is noteworthy that this is the first time such activity has been identified in lysosomes. The interaction of ADA2 with DNA lysosomes could influence, for instance, that of nucleases essential for NA detection and the regulation of the immune response, such as DNAse2,[40,41] PLD3, or PLD4.[42] Furthermore, given the flexibility of some deaminases to act on different NAs, it is possible that ADA2 also modulates the detection of lysosomal RNA (or RNA/DNA hybrids).

Our results indicate that deamination of dA residues of DNA and ADA2 influences TLR9 activation. DNA deamination is a relatively common cellular event that can be mediated by, and in the latter case is enhanced by, exposure to nitrosative compounds from the environment or nitric oxide (NO-), produced by NO synthases in phagocytes during inflammation and infection.[25] Among the DNA bases, dC is the most frequently deaminated. At the same time, spontaneous deamination of dA is a minor reaction that occurs at 2%–3% of the rate of dC deamination. Our data now suggest that this phenomenon can happen enzymatically in the lysosomes. Because dI is recognized as dG, converting dA residues in mammalian DNA could modulate the TLR9 agonist potency of DNA molecules. Of particular interest will be to investigate whether this relates to the phagocytic response, e.g., during phagocytosis of apoptotic cells and the overexposure of macrophages to self-DNA or during pathogen recognition.

Answering these questions could help improve our understanding of TLR9's mechanisms of action. Indeed, this receptor is generally believed to preferentially recognize pathogen-derived DNA containing a higher frequency of unmethylated CpG dinucleotides.[22,24] Its stimulation leads to the production of type I IFN in human pDCs.[29] However, it is unclear whether it can only recognize bacterial DNA or can also be activated by self-DNA,[43,44] just as its role on cells other than pDCs is unclear.

In this regard, although our work does not investigate the pathophysiology of DADA2, our data indicate the need to better understand the function of TLR9 in the immune response in humans. Indeed, the observation that ADA2 facilitates the activation of TLR9 might seem contradictory to the fact that its absence causes the onset of an inflammatory disease. However, a similar situation happens in many ways with DNase2 deficiency in humans. Its absence causes the onset of inflammatory disease,[41] but the enzyme facilitates TLR9 activation.[40]

In conclusion, we have shed new light on the intricate roles of ADA2 within lysosomes and its significance in lysosomal DNA sensing, enhancing our understanding of innate immunity regulation.

Limitations of the study

We have no evidence for DNA deaminase activity *in vivo* (can be proved by isolating DNA from lysosomes/cytoplasm and checking with MS/anti-inosine antibody). We do not know if the role of ADA2 in regulating NA sensing is limited to TLR9. We have not analyzed secreted ADA2.

RESOURCE AVAILABILITY

Lead contact

Further information and requests should be directed to the lead contact, Michele Proietti (proietti.michele@mhh-hannover.de).

Materials availability

All materials relevant to this manuscript are available from the lead contact with a completed materials transfer agreement.

Data and code availability

- All data reported in this paper will be shared by the lead contact upon request.
- Mass spectrometry data of the porcine brain ADA2 have been deposited to the ProteomeXchange Consortium via the PRIDE 48 partner repository with the dataset identifier PXD019373.

Figure 3. ADA2 is a lysosomal adenosine deaminase acting on DNA

(A) EndoV assay operating principle. EndoV from *Escherichia coli* (EcEndoV) cuts dI-containing DNA. The DNA is labeled with γ-^{32}P before being treated or not with EcEndoV or EcEndoV and ADA2 and visualized by phosphorimaging. C.P.1, cleaved product 1 generated by EcEndoV in the presence of dIs; C.P.2, cleaved product 2 occurs when additional (ADA2-generated) dIs are introduced.

(B) Sequences of the ODNs used.

(C) ADA2 (5 fmol) dA-to-dI activity at various pH.

(D) Top: different amounts of hrADA2 were incubated with DNA substrates at 37°C for 45 min before EcEndoV treatment. H.I., heat inactivated at 95°C for 30 min. Bottom: ADA2 (200 fmol) was incubated with DNA substrates, samples were withdrawn at different time points and treated with EcEndoV, and reaction products were analyzed as above. The DNA substrate used here contained adenosines instead of the internal inosine used above (see also B).

(E) dIs were detected by dot blot using an anti-inosine antibody.

(F) ADA2 was incubated with the indicated DNA substrates for 1 h at pH 5.5. Samples were then subjected to mass spectrometry for quantification of nucleobases. The dI levels are shown as percentage of nucleobases (top) and as dI/dA ratio (×100) (bottom).

(G) Recombinant human ADA2 (rA2) or endogenous porcine ADA2 (pA2) were incubated with ssIITI or dsAATA substrates, and after treatment with EcEndoV, samples were run on DNA sequencing gels. The length of the different fragments (in nt) is shown to the left. Multiple bands are seen in samples with pA2, likely generated by co-purifying DNases. The ADA2+EcEndoV cleavage product migrates slightly slower than 2 nt because EcEndoV produces 3′OH termini with less negative charge than 3′P termini made by DNases.

(H) Competition assays were performed by adding competitors as indicated and 20 fmol ADA2 to the reaction mixture.

(I) dA-to-dI activity of mutant ADA2 proteins (0.5–10 fmol) on various DNA substrates.

(J and K) dA-to-dI activity of increasing amount of ADA1 at pH 5.5 and 7. rA2 (5 fmoles) has been included as control (Figure 3K).

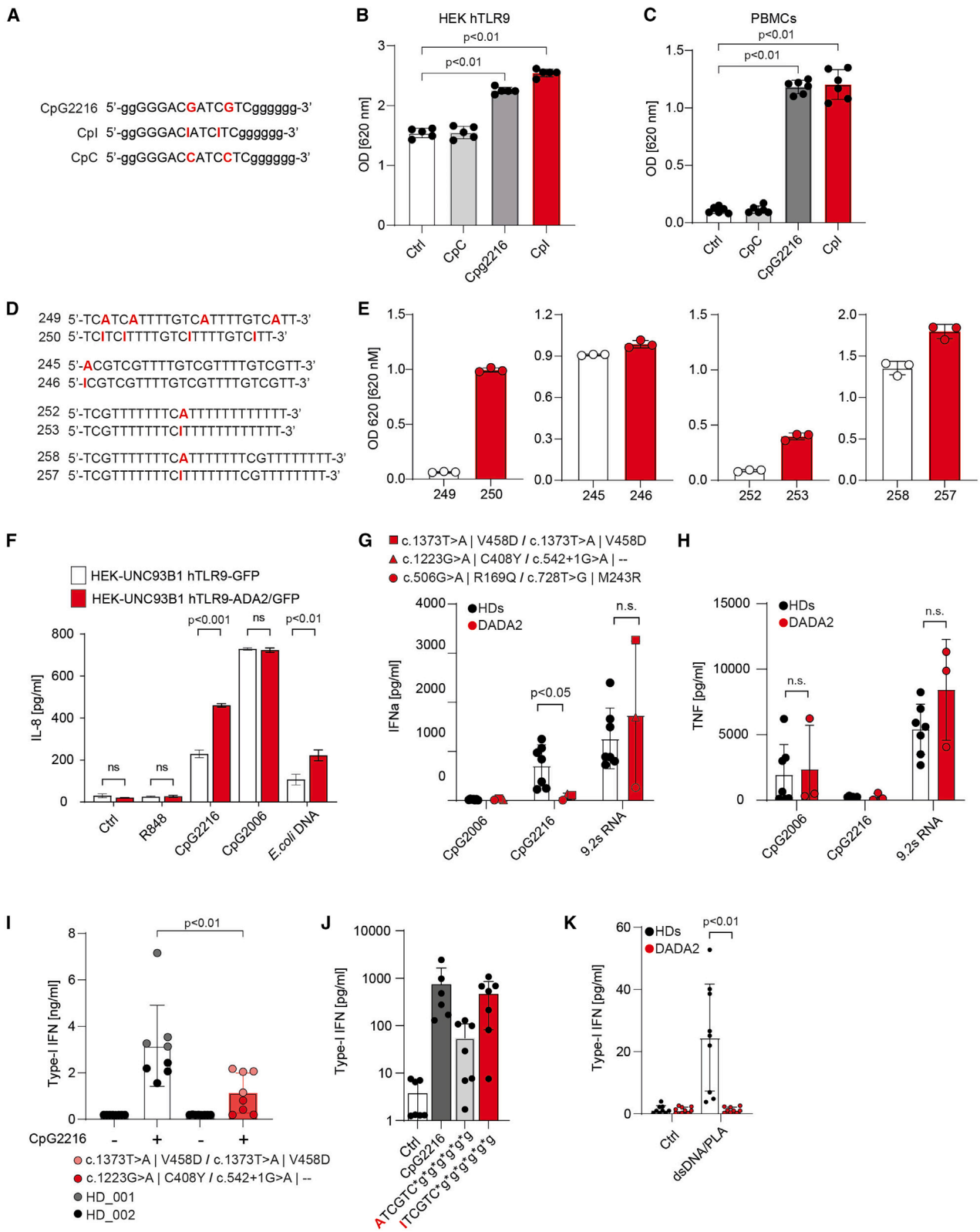

(legend on next page)

- Mass spectrometry data of the hrADA2 have been deposited to the ProteomeXchange Consortium via the PRIDE 48 partner repository with the dataset identifier PXD019382.
- This paper does not report original code.
- Any additional information required to reanalyze the data reported in this paper is available from the lead contact upon request.

ACKNOWLEDGMENTS

We thank the Center for Chronic Immunodeficiency (CCI) and the Lighthouse Core Facility (Marie Follo), both based at the University of Freiburg, and the Clinic for Rheumatology & Immunology, based at the MHH. The Deutsche Forschungsgemeinschaft (DFG) funded M.P. and B.G. under Germany's Excellence Strategy – EXC 2155 (project number 390874280). M.P. is also supported by the Deutsche Forschungsgemeinschaft (DFG) under Transregio 359 PILOT and by the Fritz Thyssen Stiftung (grant number 10.18.1.039MN). This study was also funded by the DFG (German Research Foundation) under Germany's Excellence Strategy EXC2151 390873048, of which E.B. and G.H. are members. It was also supported by the DFG (German Research Foundation) Leibniz HA 2780/10-1 to G.H., project ID 369799452 TRR237 to E.B. and G.H., project ID 397484323 TRR259 to G.H., and GRK 2168 to E.B. We also thank the patients and their families and The DADA2 Foundation.

AUTHOR CONTRIBUTIONS

M.P., M.W., I.A., E.B., and O.K.G.-T. developed the concept and designed this work. M.K., V.B., A.P., M.S., A.S., Z.A., K.A., F.I.D., K.H., A.G., C.R.S., E.T., R.L., H.E., H.S., M.M., D.S., C.V., D.G., S.B., R.G., M.P., and O.K.G.-T. performed the experiments and carried out data acquisition. M.K., M.P., I.A., M.W., and E.B. performed data analysis. B.G., G.S., and E.L. provided patient material or other reagents. B.G., P.H., and G.H. provided intellectual contributions and insightful discussions. M.P., M.W., I.A., E.B., and X.P.P. edited and revised the manuscript. All authors read and approved this manuscript.

DECLARATION OF INTERESTS

The authors declare no competing interests.

STAR★METHODS

Detailed methods are provided in the online version of this paper and include the following:

SUPPLEMENTAL INFORMATION

Supplemental information can be found online at https://doi.org/10.1016/j.celrep.2024.114899.

Figure 4. Deoxyadenosine deamination of DNA molecules and ADA2 control lysosomal DNA sensing, facilitating TLR9 activation

(A) Sequences of the CpG analogs used for stimulation experiments. CpI and CpG indicate ODNs in which the dG residues required for DNA recognition by TLR9 are replaced with dI or dC, respectively. Ctrl represents unstimulated cells.
(B) TLR9 activation was measured using human HEK-Blue TLR9 reporter cells. Cells were incubated with 5 μM of the indicated ODNs, and the magnitude of SAEP induction was measured after 20 h as an indicator of TLR9 activation.
(C) Type I IFN production by human PBMCs upon incubation with CpG analogs as in (B).
(D) Sequences of different ODNs with dA residues replaced by dI highlighted in red.
(E) Activation of TLR9 measured using human HEK-Blue TLR9 reporter cells as in (C) following stimulation with the ODNs (5 μM) described in (D).
(F) Concentration of IL-8 in the supernatant of HEK293T-hTLR-UNC93B1 reporter cells after overnight stimulation with the indicated compounds.
(G and H) IFN-α (G) and TNF (H) were measured by ELISA in the supernatants of PBMCs from healthy donors and DADA2 patients after overnight stimulation with the indicated compounds. Three DADA2 patients with the indicated genotype and three age- and gender-matched healthy donors have been compared.
(I) Type I IFN measured by HEK-type I IFN reporter cells in the supernatants of sorted pDCs from healthy donors or DADA2 patients after overnight stimulation with CpG2216.
(J) Type I IFN was measured by HEK-type I IFN reporter cells in the supernatants of PBMCs from healthy individuals after overnight stimulation with the indicated ODN.
(K) Type-I IFN production by PBMCs from healthy donors or DADA2 patients upon lysosomal sensing of dsDNA.
Unpaired t test (in B, C, G, H, K) and ANOVA t test (in F) were used to calculate *p* values.

Received: December 13, 2023
Revised: September 19, 2024
Accepted: October 7, 2024

REFERENCES

1. Schrader, W.P., Pollara, B., and Meuwissen, H.J. (1978). Characterization of the residual adenosine deaminating activity in the spleen of a patient with combined immunodeficiency disease and adenosine deaminase deficiency. Proc. Natl. Acad. Sci. USA *75*, 446–450. https://doi.org/10.1073/pnas.75.1.446.
2. Daddona, P.E., and Kelley, W.N. (1981). Characteristics of an aminohydrolase distinct from adenosine deaminase in cultured human lymphoblasts. Biochim. Biophys. Acta *658*, 280–290. https://doi.org/10.1016/0005-2744(81)90298-9.
3. Ratech, H., and Hirschhorn, R. (1981). Serum adenosine deaminase in normals and in a patient with adenosine deaminase deficient-severe combined immunodeficiency. Clin. Chim. Acta *115*, 341–347. https://doi.org/10.1016/0009-8981(81)90247-3.
4. Iwaki-Egawa, S., Yamamoto, T., and Watanabe, Y. (2006). Human plasma adenosine deaminase 2 is secreted by activated monocytes. Biol. Chem. *387*, 319–321. https://doi.org/10.1515/BC.2006.042.
5. Zavialov, A.V., Gracia, E., Glaichenhaus, N., Franco, R., Zavialov, A.V., and Lauvau, G. (2010). Human adenosine deaminase 2 induces differentiation of monocytes into macrophages and stimulates proliferation of T helper cells and macrophages. J. Leukoc. Biol. *88*, 279–290. https://doi.org/10.1189/jlb.1109764.
6. Teresa, K., Tarrant, S.J.K., and Hershfield, M.S. (2021). Elucidating the pathogenesis of adenosine deaminase 2 deficiency: current status and unmet needs. Expert Opin. Orphan Drugs *9*. https://doi.org/10.1080/21678707.2021.2050367.
7. Flinn, A.M., and Gennery, A.R. (2018). Adenosine deaminase deficiency: a review. Orphanet J. Rare Dis. *13*, 65. https://doi.org/10.1186/s13023-018-0807-5.
8. Giblett, E.R., Anderson, J.E., Cohen, F., Pollara, B., and Meuwissen, H.J. (1972). Adenosine-deaminase deficiency in two patients with severely impaired cellular immunity. Lancet *2*, 1067–1069. https://doi.org/10.1016/s0140-6736(72)92345-8.
9. Hashem, H., Kelly, S.J., Ganson, N.J., and Hershfield, M.S. (2017). Deficiency of Adenosine Deaminase 2 (DADA2), an Inherited Cause of Polyarteritis Nodosa and a Mimic of Other Systemic Rheumatologic Disorders. Curr. Rheumatol. Rep. *19*, 70. https://doi.org/10.1007/s11926-017-0699-8.
10. Navon Elkan, P., Pierce, S.B., Segel, R., Walsh, T., Barash, J., Padeh, S., Zlotogorski, A., Berkun, Y., Press, J.J., Mukamel, M., et al. (2014). Mutant Adenosine Deaminase 2 in a Polyarteritis Nodosa Vasculopathy. N. Engl. J. Med. *370*, 921–931. https://doi.org/10.1056/NEJMoa1307362.
11. Zhou, Q., Yang, D., Ombrello, A.K., Zavialov, A.V., Toro, C., Zavialov, A.V., Stone, D.L., Chae, J.J., Rosenzweig, S.D., Bishop, K., et al. (2014). Early-Onset Stroke and Vasculopathy Associated with Mutations in ADA2. N. Engl. J. Med. *370*, 911–920. https://doi.org/10.1056/NEJMoa1307361.
12. Bartok, E., and Hartmann, G. (2020). Immune Sensing Mechanisms that Discriminate Self from Altered Self and Foreign Nucleic Acids. Immunity *53*, 54–77. https://doi.org/10.1016/j.immuni.2020.06.014.
13. Schlee, M., and Hartmann, G. (2016). Discriminating self from non-self in nucleic acid sensing. Nat. Rev. Immunol. *16*, 566–580. https://doi.org/10.1038/nri.2016.78.
14. Collin, M., McGovern, N., and Haniffa, M. (2013). Human dendritic cell subsets. Immunology *140*, 22–30. https://doi.org/10.1111/imm.12117.
15. Coutinho, M.F., Prata, M.J., and Alves, S. (2012). Mannose-6-phosphate pathway: a review on its role in lysosomal function and dysfunction. Mol. Genet. Metab. *105*, 542–550. https://doi.org/10.1016/j.ymgme.2011.12.012.
16. Sleat, D.E., Wang, Y., Sohar, I., Lackland, H., Li, Y., Li, H., Zheng, H., and Lobel, P. (2006). Identification and validation of mannose 6-phosphate glycoproteins in human plasma reveal a wide range of lysosomal and non-lysosomal proteins. Mol. Cell. Proteomics *5*, 1942–1956. https://doi.org/10.1074/mcp.M600030-MCP200.
17. Zavialov, A.V., and Engström, A. (2005). Human ADA2 belongs to a new family of growth factors with adenosine deaminase activity. Biochem. J. *391*, 51–57. https://doi.org/10.1042/BJ20050683.
18. Zavialov, A.V., Yu, X., Spillmann, D., Lauvau, G., and Zavialov, A.V. (2010). Structural Basis for the Growth Factor Activity of Human Adenosine Deaminase ADA2. J. Biol. Chem. *285*, 12367–12377. https://doi.org/10.1074/jbc.M109.083527.
19. Yan, Y., Zhang, D., Zhou, P., Li, B., and Huang, S.Y. (2017). HDOCK: a web server for protein-protein and protein-DNA/RNA docking based on a hybrid strategy. Nucleic Acids Res. *45*, W365–W373. https://doi.org/10.1093/nar/gkx407.
20. Blair, R.H., Goodrich, J.A., and Kugel, J.F. (2013). Using FRET to monitor protein-induced DNA bending: the TBP-TATA complex as a model system. Methods Mol. Biol. *977*, 203–215. https://doi.org/10.1007/978-1-62703-284-1_16.
21. Ahmad-Nejad, P., Häcker, H., Rutz, M., Bauer, S., Vabulas, R., and Wagner, H. (2002). Bacterial CpG-DNA and lipopolysaccharides activate Toll-like receptors at distinct cellular compartments. Eur. J. Immunol. *32*, 1958–1968. https://doi.org/10.1002/1521-4141(200207)32:7<1958::AID-IMMU1958>3.0.CO;2-U.
22. Bauer, S., Kirschning, C.J., Häcker, H., Redecke, V., Hausmann, S., Akira, S., Wagner, H., and Lipford, G.B. (2001). Human TLR9 confers responsiveness to bacterial DNA via species-specific CpG motif recognition. Proc. Natl. Acad. Sci. USA *98*, 9237–9242. https://doi.org/10.1073/pnas.161293498.
23. Hemmi, H., Takeuchi, O., Kawai, T., Kaisho, T., Sato, S., Sanjo, H., Matsumoto, M., Hoshino, K., Wagner, H., Takeda, K., and Akira, S. (2000). A Toll-like receptor recognizes bacterial DNA. Nature *408*, 740–745. https://doi.org/10.1038/35047123.
24. Krieg, A.M. (2002). CpG motifs in bacterial DNA and their immune effects. Annu. Rev. Immunol. *20*, 709–760. https://doi.org/10.1146/annurev.immunol.20.100301.064842.
25. Alseth, I., Dalhus, B., and Bjørås, M. (2014). Inosine in DNA and RNA. Curr. Opin. Genet. Dev. *26*, 116–123. https://doi.org/10.1016/j.gde.2014.07.008.
26. Kerkmann, M., Rothenfusser, S., Hornung, V., Towarowski, A., Wagner, M., Sarris, A., Giese, T., Endres, S., and Hartmann, G. (2003). Activation with CpG-A and CpG-B oligonucleotides reveals two distinct regulatory pathways of type I IFN synthesis in human plasmacytoid dendritic cells. J. Immunol. *170*, 4465–4474. https://doi.org/10.4049/jimmunol.170.9.4465.
27. Pelka, K., Bertheloot, D., Reimer, E., Phulphagar, K., Schmidt, S.V., Christ, A., Stahl, R., Watson, N., Miyake, K., Hacohen, N., et al. (2018). The Chaperone UNC93B1 Regulates Toll-like Receptor Stability Independently of Endosomal TLR Transport. Immunity *48*, 911–922.e7. https://doi.org/10.1016/j.immuni.2018.04.011.
28. Hartmann, G., and Krieg, A.M. (2000). Mechanism and function of a newly identified CpG DNA motif in human primary B cells. J. Immunol. *164*, 944–953. https://doi.org/10.4049/jimmunol.164.2.944.
29. Krug, A., Rothenfusser, S., Hornung, V., Jahrsdörfer, B., Blackwell, S., Ballas, Z.K., Endres, S., Krieg, A.M., and Hartmann, G. (2001). Identification of CpG oligonucleotide sequences with high induction of IFN-alpha/beta in plasmacytoid dendritic cells. Eur. J. Immunol. *31*, 2154–2163. https://doi.org/10.1002/1521-4141(200107)31:7<2154::aid-immu2154>3.0.co;2-u.
30. Hornung, V., Guenthner-Biller, M., Bourquin, C., Ablasser, A., Schlee, M., Uematsu, S., Noronha, A., Manoharan, M., Akira, S., de Fougerolles, A., et al. (2005). Sequence-specific potent induction of IFN-alpha by short

interfering RNA in plasmacytoid dendritic cells through TLR7. Nat. Med. *11*, 263–270. https://doi.org/10.1038/nm1191.

31. Ostendorf, T., Zillinger, T., Andryka, K., Schlee-Guimaraes, T.M., Schmitz, S., Marx, S., Bayrak, K., Linke, R., Salgert, S., Wegner, J., et al. (2020). Immune Sensing of Synthetic, Bacterial, and Protozoan RNA by Toll-like Receptor 8 Requires Coordinated Processing by RNase T2 and RNase 2. Immunity *52*, 591–605.e6. https://doi.org/10.1016/j.immuni.2020.03.009.
32. Saghiri, R., Ghashghai, N., Movaseghi, S., Poursharifi, P., Jalilfar, S., Bidhendi, M.A., Ghazizadeh, L., and Ebrahimi-Rad, M. (2012). Serum adenosine deaminase activity in patients with systemic lupus erythematosus: a study based on ADA1 and ADA2 isoenzymes pattern. Rheumatol. Int. *32*, 1633–1638. https://doi.org/10.1007/s00296-011-1836-8.
33. Bowers, S.M., Ng, B., Abdossamadi, S., Kariminia, A., Cabral, D.A., Cuvelier, G.D.E., Schultz, K.R., and Brown, K.L. (2023). Elevated ADA2 Enzyme Activity at the Onset of Chronic Graft-versus-Host Disease in Children. Transplant. Cell. Ther. *29*, 303.e1–303.e9. https://doi.org/10.1016/j.jtct.2023.02.014.
34. Salesi, M., Ghazvini, R.A., Farajzadegan, Z., Karimifar, M., Karimzadeh, H., Masoumi, M., and Ebrahimi, B. (2012). Serum adenosine deaminase in patients with rheumatoid arthritis treated with methotrexate. J. Res. Pharm. Pract. *1*, 72–76. https://doi.org/10.4103/2279-042X.108374.
35. Gakis, C. (1996). Adenosine deaminase (ADA) isoenzymes ADA1 and ADA2: diagnostic and biological role. Eur. Respir. J. *9*, 632–633. https://doi.org/10.1183/09031936.96.09040632.
36. Zheng, Y., Lorenzo, C., and Beal, P.A. (2017). DNA editing in DNA/RNA hybrids by adenosine deaminases that act on RNA. Nucleic Acids Res. *45*, 3369–3377. https://doi.org/10.1093/nar/gkx050.
37. Rubio, M.A.T., Pastar, I., Gaston, K.W., Ragone, F.L., Janzen, C.J., Cross, G.A.M., Papavasiliou, F.N., and Alfonzo, J.D. (2007). An adenosine-to-inosine tRNA-editing enzyme that can perform C-to-U deamination of DNA. Proc. Natl. Acad. Sci. USA *104*, 7821–7826. https://doi.org/10.1073/pnas.0702394104.
38. Nishida, K., Arazoe, T., Yachie, N., Banno, S., Kakimoto, M., Tabata, M., Mochizuki, M., Miyabe, A., Araki, M., Hara, K.Y., et al. (2016). Targeted nucleotide editing using hybrid prokaryotic and vertebrate adaptive immune systems. Science *353*, aaf8729. https://doi.org/10.1126/science.aaf8729.
39. Komor, A.C., Kim, Y.B., Packer, M.S., Zuris, J.A., and Liu, D.R. (2016). Programmable editing of a target base in genomic DNA without double-stranded DNA cleavage. Nature *533*, 420–424. https://doi.org/10.1038/nature17946.
40. Chan, M.P., Onji, M., Fukui, R., Kawane, K., Shibata, T., Saitoh, S.i., Ohto, U., Shimizu, T., Barber, G.N., and Miyake, K. (2015). DNase II-dependent DNA digestion is required for DNA sensing by TLR9. Nat. Commun. *6*, 5853. https://doi.org/10.1038/ncomms6853.
41. Rodero, M.P., Tesser, A., Bartok, E., Rice, G.I., Della Mina, E., Depp, M., Beitz, B., Bondet, V., Cagnard, N., Duffy, D., et al. (2017). Type I interferon-mediated autoinflammation due to DNase II deficiency. Nat. Commun. *8*, 2176. https://doi.org/10.1038/s41467-017-01932-3.
42. Gavin, A.L., Huang, D., Huber, C., Mårtensson, A., Tardif, V., Skog, P.D., Blane, T.R., Thinnes, T.C., Osborn, K., Chong, H.S., et al. (2018). PLD3 and PLD4 are single-stranded acid exonucleases that regulate endosomal nucleic-acid sensing. Nat. Immunol. *19*, 942–953. https://doi.org/10.1038/s41590-018-0179-y.
43. Boule, M.W., Broughton, C., Mackay, F., Akira, S., Marshak-Rothstein, A., and Rifkin, I.R. (2004). Toll-like receptor 9-dependent and -independent dendritic cell activation by chromatin-immunoglobulin G complexes. J. Exp. Med. *199*, 1631–1640. https://doi.org/10.1084/jem.20031942.
44. Leadbetter, E.A., Rifkin, I.R., Hohlbaum, A.M., Beaudette, B.C., Shlomchik, M.J., and Marshak-Rothstein, A. (2002). Chromatin-IgG complexes activate B cells by dual engagement of IgM and Toll-like receptors. Nature *416*, 603–607. https://doi.org/10.1038/416603a.
45. von Schoenfeld, A., Bronsert, P., Poc, M., Fuller, A., Filby, A., Kraft, S., Kurowski, K., Sörensen, K., Huber, J., Pfeiffer, J., et al. (2021). Multiple Immunostainings with Different Epitope Retrievals-The FOLGAS Protocol. Int. J. Mol. Sci. *23*, 223. https://doi.org/10.3390/ijms23010223.
46. Schrodinger, L.L.C. (2015). The PyMOL Molecular Graphics System version 3.0. https://doi.org/10.1093/nar/gkx407.
47. Perez-Riverol, Y., Csordas, A., Bai, J., Bernal-Llinares, M., Hewapathirana, S., Kundu, D.J., Inuganti, A., Griss, J., Mayer, G., Eisenacher, M., et al. (2019). The PRIDE database and related tools and resources in 2019: improving support for quantification data. Nucleic Acids Res. *47*, D442–D450. https://doi.org/10.1093/nar/gky1106.
48. Yang, W., Shah, P., Toghi Eshghi, S., Yang, S., Sun, S., Ao, M., Rubin, A., Jackson, J.B., and Zhang, H. (2014). Glycoform analysis of recombinant and human immunodeficiency virus envelope protein gp120 via higher energy collisional dissociation and spectral-aligning strategy. Anal. Chem. *86*, 6959–6967. https://doi.org/10.1021/ac500876p.
49. Keer, N., Hershfield, M., Caskey, T., and Unizony, S. (2016). Novel compound heterozygous variants in CECR1 gene associated with childhood onset polyarteritis nodosa and deficiency of ADA2. Rheumatology *55*, 1145–1147.
50. Lee, P.Y., Kellner, E.S., Huang, Y., Furutani, E., Huang, Z., Bainter, W., Alosaimi, M.F., Stafstrom, K., Platt, C.D., Stauber, T., et al. (2020). Genotype and functional correlates of disease phenotype in deficiency of adenosine deaminase 2 (DADA2). J. Allergy Clin. Immunol. *145*, 1664–1672.e10. https://doi.org/10.1016/j.jaci.2019.12.908.
51. Hashem, H., Kumar, A.R., Müller, I., Babor, F., Bredius, R., Dalal, J., Hsu, A.P., Holland, S.M., Hickstein, D.D., Jolles, S., et al. (2017). Hematopoietic stem cell transplantation rescues the hematological, immunological, and vascular phenotype in DADA2. Blood *130*, 2682–2688.
52. Caorsi, R., Penco, F., Grossi, A., Insalaco, A., Omenetti, A., Alessio, M., Conti, G., Marchetti, F., Picco, P., Tommasini, A., et al. (2017). ADA2 deficiency (DADA2) as an unrecognised cause of early onset polyarteritis nodosa and stroke: a multicentre national study. Ann. Rheum. Dis. *76*, 1648–1656.
53. Belot, A., Wassmer, E., Twilt, M., Lega, J.-C., Zeef, L.A., Oojageer, A., Kasher, P.R., Mathieu, A.-L., Malcus, C., Demaret, J., et al. (2014). Mutations in CECR1 associated with a neutrophil signature in peripheral blood. Pediatr. Rheumatol. Online J *24*, 44. https://doi.org/10.1186/1546-0096-12-44.

STAR★METHODS

KEY RESOURCES TABLE

REAGENT or RESOURCE	SOURCE	IDENTIFIER
Antibodies		
Rabbit monoclonal anti-Human CD14	Biogenex	Cat#AN814GP
Rabbit polyclonal anti-human CECR1	Sigma-Aldrich	Cat#HPA007888; RRID:AB_1078495
Mouse monoclonal anti-human CD107a (LAMP1)	Thermo Fisher Scientific	Cat#14-1079-80; RRID:AB_467426
Rabbit monoclonal anti-human LAMP1	Cell Signaling Technology	Cat#58996; RRID:AB_2927691
Goat polyclonal secondary anti-rabbit	Thermo Fisher Scientific	Cat#A-11010; RRID:AB_2534077
Mouse monoclonal anti-human CD3	Biolegend	Cat#317306; RRID:AB_571907
Mouse monoclonal anti-human CD14	Biolegend	Cat# 367116; RRID:AB_2571928
Mouse monoclonal anti-human CD16	Biolegend	Cat#302006; RRID:AB_314206
Mouse monoclonal anti-human CD19	BD Biosciences	Cat#555412; RRID:AB_395812
Rat monoclonal anti-human CD4	Biolegend	Cat#357404; RRID:AB_2562035
Mouse monoclonal anti-human CD11c	Biolegend	Cat#301628; RRID:AB_10898313
Mouse monoclonal anti-human HLA-DR	Biolegend	Cat#307610; RRID:AB_314688
Mouse monoclonal anti-human CD4	Biolegend	Cat#300518; RRID:AB_314086
Mouse monoclonal anti-human CD11c	Biolegend	Cat#301628; RRID:AB_10898313
Mouse monoclonal anti-human HLA-DR	Biolegend	Cat#307616; RRID:AB_493588
Rabbit polyclonal anti-Inosine	MbIbio	Cat#PM098
Goat anti-Rabbit IgG	Vectorlabs	Cat#PI-1000-1
Bacterial and virus strains		
pET28b	Novagen	cat#69865
pET28b-EcEndoV		N/A
E.coli	NEB	Cat#C2566
Biological samples		N/A
PBMCs from healthy volunteers		N/A
PBMCs from DADA2 patients		N/A
Chemicals, peptides, and recombinant proteins		
SuperfrostPlus	Langenbrinck	Cat#03-0060
Biotin blocking reagent	Agilent Dako	Cat#X0590
Dako REAL Detection System	Agilent Dako	Cat#K5005
StayBlue/AP	Abcam	Cat#ab176915
Streptavidin Alexa Fluor 488 Conjugate	Thermo Fisher Scientific	Cat#S32354
Streptavidin Alexa Fluor 555	Thermo Fisher Scientific	Cat#S32355
DAPI	Thermo Fisher Scientific	Cat#62248
PAN Biotech	Pancoll human	Cat#P04-60500
Normal goat serum	Abcam	Cat#ab7481
PEI MAX	Polysciences	Cat#24765-1
M11V3 media	Bioconcept	Cat#V3-k
Ni-NTA-Agarose	Qiagen	Cat#30230
Nickel Sepharose	GE Healthcare	Cat#17-5248-02
DNA gel loading dye	Thermo Fisher Scientific	Cat# R0611
T4 polynucleotide kinase	New England Biolabs	Cat# M0201
Supersignal West Femto Maximum Sensitivity Substrate	Thermo Fisher Scientific	Cat# 34094
Deaminase inhibitor EHNA	Sigma-Aldrich	Cat# E114
Benzonase	Santa Cruz Biotech	Cat#sc-391121B

(*Continued on next page*)

Continued

REAGENT or RESOURCE	SOURCE	IDENTIFIER
Nuclease P1	Sigma-Aldrich	Cat#N8630
Alkaline phosphatase	Sigma-Aldrich	Cat#P5931
Deoxycoformicin	Sigma-Aldrich	Cat#116860
MIB super buffer 2	Jena Bioscience	Cat#CS-332
MIB super buffer 1	Jena Bioscience	Cat#CS-332
Blasticidin	Invivogen	Cat#ant-bl-05
Zeocin	Invivogen	Cat#ant-zn-05
QUANTI-Blue solution	Invivogen	Cat#rep-qbs
Biotin blocking reagent	Agilent Dako	Cat#X0590
E.coli Endonuclease V	Produced and purified in-house	EcEndoV
Human Endonuclease V	Produced and purified in-house	hEndoV
Superdex75 column	GE Healthcare	Cat#28-9893-33
TransIT®-LT1	Mirus Bio	Cat#731-0027
DOTAP	Carl Roth	Cat# L787.3
Purified E. coli DNA	Invitrogen	Cat#tlrl-ecdna
Critical commercial assays		
Dako REAL Detection System	Dako Agilent	Cat#K5005
CD14 MicroBeads, human	Miltenyi	Cat#130-050-201
DNaseAlert QC System 480 assays	Thermo Fisher Scientific	Cat#AM1970
Adenosine Deaminase (ADA) Test Kit	Diazyme	Cat#DZ117A-K
JBScreen Thermofluor	Jena bioscience	Cat# CS-332
BD OptEIA™ Human TNF ELISA Set	BD Biosciences	Cat# 555212
BD OptEIA™ Human IL-8 ELISA Set	BD Biosciences	Cat# 555244
IFN-a module ELISA Set	Thermo Fischer Scientific	Cat#BMS216C, Cat#BMS216MSTK, Cat#BMS216MSTS
Experimental models: Cell lines		
Human TLR9 Reporter HEK293 Cells (NF-κB)	Invivogen	hkb-htlr9
HEK-Blue™ IFN-α/β cells	Invivogen	hkb-ifnabv2
293XL/hTLR7-HA cell line (Invivogen) with human UNC93B1-mCitrine WT	Pelka et al.[27]	N/A
293XL/hTLR9-HA cell line (Invivogen) with human UNC93B1-mCitrine WT	Pelka et al.[27]	N/A
Oligonucleotides		
ggGGGACGATCGTCgggggg	Biomers	CpG2216
ggGGGACCATCCTCgggggg	Biomers	CpC
ggGGGACIATCITCgggggg	Biomers	CpI
ACTGGACAIITICTCCGAGG	Eurofins	IITI
CCTCGGAGTITTTGTCCAGT	Eurofins	IITI-comp
ACTGGACAAATACTCCGAGG	Eurofins	AATA
CCTCGGAGTATTTGTCCAGT	Eurofins	AATA-comp
GCTGGACAAATACTCCGAGG	Eurofins	A1mut
ATGGGATATACCGGCGACGCATGATGAACA	Eurofins	CompC
TGTTCATCATGCGTCGCCGGTATATCCCA	Eurofins	CompCCS
TGTTCATCATGCGTCGCCGGTATATCCCAT	Eurofins	CompCC
ACCGACCACGCACTGCGCGTTTT CGCGCTATTCCAGAGTTGA	Eurofins	HpTT42
ACCGACCACGCACTGCACGTTTTCG TGCTATTCCAGAGTTGA	Eurofins	HpTTStemAT42

(*Continued on next page*)

Continued

REAGENT or RESOURCE	SOURCE	IDENTIFIER
TCCGACCACGCACTGCGCGTAATCG CGCTATTCCAGAGTTGT	Eurofins	HpAA42
ACCACGCACTGCGCGTTTTCGCG CTATTCCAGAG	Eurofins	Hp34
ACGCACTGCGCGTTTTCGCGCTATTCCA	Eurofins	Hp28
GCACTGCGCGTTTTCGCGCTATTC	Eurofins	Hp24
ACTGCGCGTTTTCGCGCTAT	Eurofins	Hp20
TGGCTGGTGCGTGAATAAGGTCTCAACT	Eurofins	Hairpin-comp
GGATACGTAACAACGCTTATGCATCGC CGCCGCTACATCCCTGAGCTGAC	Eurofins	50bpO
TGTGTTCGATCTCGATCAGAATGACG ATGCATAAGCGTTGTTACGTATCC	Eurofins	50bpO-c-PY
GTCAGCTCAGGGATGTAGCGGCGG	Eurofins	50bpO-c-Fl
GGGGGACGATCGTCGGGGGG	Eurofins	CpG2216
TGGGATATACCGGCG	Eurofins	A15
ACGCATGATGAACA	Eurofins	B14
TGGGATATACCGGC	Eurofins	A14
ACGCATGATGAAC	Eurofins	B13
ACGTCGTTTTGTCGTTTTGTCGTT	Biomers	245
ICGTCGTTTTGTCGTTTTGTCGTT	Biomers	246
TCATCATTTTGTCATTTTGTCATT	Biomers	249
TCITCITTTTGTCITTTTGTCITT	Biomers	250
TCGTTTTTTTCATTTTTTTTTTTT	Biomers	252
TCGTTTTTTTCITTTTTTTTTTT	Biomers	253
TCGTTTTTTTCITTTTTTTCGTTTTTTTT	Biomers	257
TCGTTTTTTTCATTTTTTTCGTTTTTTTT	Biomers	258
rArGrCrUrUrArArCrCrUrGrUrCrCrUrUrCrArA[30]	Biomers	9.2 sRNA
Recombinant DNA		
pLenti-IRES-GFP-Puro	Jonas Doerr, Institute of Reconstructive Neurobiology, University of Bonn	N/A
pLenti-ADA2-IRES-GFP-Puro	This paper	N/A
Software and algorithms		
ZEISS ZEN 3.9	ZEISS	https://www.micro-shop.zeiss.com/
IMARIS v9.1	Oxford Instruments	https://imaris.oxinst.com/
ImageJ/FiJi		https://imagej.net/software/fiji/
UCSF Chimera		N/A
Proteome Discoverer 1.4		N/A
MaxQuant v1.5.3.54		N/A
ImageQuant IQTL 8.2		N/A
PyMOL		N/A
GraphPad Prism 10	GraphPad Software	https://www.graphpad.com/scientific-software/prism/
Other		
Mass spec data of the porcine brain ADA2		PXD019373
Mass spec data of the human recombinant ADA2		PXD019382

EXPERIMENTAL MODEL AND STUDY PARTICIPANT DETAILS

Human samples

For microscopy, human palatine tonsils were obtained after a positive ethical vote by local authorities (251/13_140389, Ethikkommission der Albert-Ludwigs-Universität Freiburg, Freiburg, Germany).

For experiments with cells from healthy individuals and DADA2 patients, blood was obtained after a positive ethical vote by local authorities (322/15, Ethikkommission der Albert-Ludwigs-Universität Freiburg, Freiburg, Germany).

METHOD DETAILS

Cell culture

Human TLR9 Reporter HEK293 Cells (NF-κB) and HEK-Blue IFN- α/β cells were maintained in DMEM, 4.5 g/L glucose, 10% (v/v) fetal bovine serum (FBS), 100 U/ml penicillin, 100 μg/mL streptomycin, 2 mM L-glutamine, 10 μg/mL of blasticidin and 100 μg/mL of zeocin.

293XL/hTLR7-HA cell line (Invivogen) and 293XL/hTLR9-HA cell line (Invivogen) both expressing human UNC93B1-mCitrine WT[27] were maintained in DMEM, 4.5 g/L glucose, 10% (v/v) FBS, 100 U/ml penicillin, 100 μg/mL streptomycin and 2 mM L-glutamine.

Immunohistochemistry of human tonsils

For histopathological sample analysis, 2 μm sections were taken from buffered formalin fixed paraffin embedded biopsies of human palatine tonsils after positive ethical vote by local authorities (251/13_140389, Ethikkommission der Albert-Ludwigs-Universität Freiburg, Freiburg, Germany) and put on coated slides (SuperfrostPlus, Langenbrinck, Emmendingen, Germany, cat. # 03–0060). Deparaffinization was done in xylene, followed by 100% ethanol, with a concentration decreasing in aqueous solution until 50% was reached, followed by distilled water. Blocking endogenous biotin (Biotin blocking reagent, Agilent Dako, Glostrup, Denmark, cat. #X0590) was performed before any primary antibodies. Staining was done with a primary antibody against CD14 (rabbit monoclonal antibody, clone EP128, BioGenex, Fremont, USA; cat. # AN814GP; dilution 1:100); no antigen retrieval was necessary. Secondary antibodies were in a ready-to-use (RTU) formulation and incubated afterward (Dako REAL Detection System, Agilent Dako, cat. #K5005; containing a mixture of biotinylated goat-anti mouse and goat-anti rabbit antibodies) and visualized with an alkaline phosphatase based red chromogen reaction from the same kit, according to the manufacturer's guidelines. After denaturation of the first antibodies as described,[45] heat-mediated epitope retrieval in a steamer for 30 min in Tris-buffered saline at pH 6.1, followed by staining against ADA2 (anti-CECR1 rabbit polyclonal antibody, Sigma-Aldrich, cat. # HPA007888, dilution 1:80). The secondary antibodies were again taken from the kit, visualized by an alkaline phosphatase based blue chromogen reaction (StayBlue/AP, Abcam, Cambridge, UK, cat. # ab176915). Photos were taken with an Olympus BX 51 microscope (Olympus Hamburg, Germany) with the AxioCam MRc microscope camera (Carl Zeiss, Oberkochen, Germany).

Immunofluorescence of human tonsils

For immunofluorescence, 2 μm sections were taken from buffered formalin fixed paraffin embedded biopsies of human palatine tonsils after positive ethical vote by local authorities (251/13_140389, Ethikkommission der Albert-Ludwigs-Universität Freiburg, Freiburg, Germany) and put on coated slides (SuperfrostPlus, Langenbrinck, Emmendingen, Germany, cat. # 03–0060). Subsequent staining was done following the protocol described by von Schoenfeld et al..[45] The first staining step was done against LAMP1 (mouse monoclonal antibody, clone eBioH4A3, Thermo Fisher Scientific, cat. # 14-1079-80, dilution 1:100) after heat mediated epitope retrieval in a steamer for 30 min in Tris-buffered saline at pH 6.1, visualized in the 488 channel (RTU secondary antibodies from the kit as mentioned above, coupled to Streptavidin Alexa Fluor 488 Conjugate, Thermo Fisher Scientific; cat. #S32354, dilution 1:200). The second staining step was done against ADA2 (anti-CECR1 rabbit polyclonal antibody, Sigma-Aldrich, cat. # HPA007888, dilution 1:80) and high pressure cooking epitope retrieval for 2 min in citric buffer pH 6, visualized in the 555 channel (RTU secondary antibodies from the kit as mentioned above, coupled to Streptavidin Alexa Fluor 555 Conjugate, Thermo Fisher Scientific; cat. #S32355 dilution 1:200). Nuclei were counterstained with DAPI (Thermo Fisher Scientific; cat. # 62248, dil: 1:1000). Photos were taken with a fluorescence microscope (Axioplan 2, Zeiss) with the AxioCam MRm microscope camera.

Monocytes isolation from peripheral blood mononuclear cells

Peripheral blood mononuclear cells (PBMC) were prepared by centrifugation on a Pancoll gradient (PAN Biotech, Pancoll human cat. #P04-60500). Blood $CD14^+$ monocytes were isolated from DADA2 patients (ethical vote 322/15, Ethikkommission der Albert-Ludwigs-Universität Freiburg, Freiburg, Germany) or healthy donors' PBMC by positive selection using magnetic beads (Miltenyi, cat. # 130-050-201) according to the manufacturer's protocol. Monocytes purity was 95%–98% as measured by flow cytometry.

Immunofluorescence of primary monocytes from peripheral blood of healthy donors and DADA2 patients

Monocytes were isolated from the blood of healthy donors, as described above. 150.000 cells were seeded in RPMI per well in a chambered coverslip (IBIDI: cat. # 80826) and let settle for 2 h at 37°C in the incubator. After incubation, RPMI was removed, and cells were washed three times with PBS before fixation with precooled (−20°C) 1:1 acetone/methanol fixative for 30 min at −20°C. Afterward, the fixative was aspirated, and the sample was washed three times in PBS for 5 min. The cells were subsequently permeabilized in PBS with 10% normal goat serum (NGS) (Abcam, cat. # ab7481) and 0.05% Tween (PanReac AppliChem, cat. # A4974) for 10 min. After permeabilization, the cells were blocked in blocking solution (PBS with 10% NGS +0.05% Tween 20) for >2 h at RT. Hereafter, cells were immunostained with a rabbit anti-human CECR1 (Sigma cat. # HPA007888; 1:100 in blocking solution) and anti-LAMP1-AF488 (Cell Signaling, cat. # 58996, diluted 1:200, in blocking solution) overnight at 4°C. After incubation,

cells were washed three times in PBS before being incubated with goat anti-rabbit AF546 (Thermo Fisher Scientific, cat. # A-11010, 1:500) and DAPI (Thermo Fisher Scientific; cat. # 62248, dil: 1:1000) in DPBS with 10% NGS and 0.05% Tween 20 for 1 h at RT. The slides were mounted with Dako mounting medium (Agilent Technologies cat. #S302380-2). The images were taken with the LSM880 (Zeiss) and analyzed with ZEN (Zeiss) and ImageJ/FiJi2. The software Imaris v9.1 (Oxford Instruments) was used for the 3D reconstruction, profile plots, and co-localization. For the quantification of LAMP1 and ADA2 in peripheral monocytes, the Coloc tool from IMARIS was used. The tool allows defining thresholds with FMO or 2nd Ab-only control stainings for each experiment. Defining that threshold, IMARIS renders the region of interest for single- or co-localizing stainings. The newly created ''colocalizing'' channel can then be quantified, i.e., the number of colocalizing voxels. We performed the same steps with ADA2 and DAPI as internal negative control.

Plasmacytoid and conventional dendritic cells isolation from peripheral blood mononuclear cells for immunofluorescence

Peripheral blood mononuclear cells (PBMC) were prepared by centrifugation on a Pancoll gradient (PAN Biotech, Pancoll human cat. #P04-60500). Plasmacytoid dendritic cells (pDCs) were sorted as lineage (CD3-FITC, CD14-FITC, CD16-FITC, CD19-FITC)$^{-}$, HLA-DR-PE-Cy7^{+}, CD11c-BV421^{dim}, CD4-ACP-Cy7^{high}, conventional DC (cDCs) as lineage (CD3-FITC, CD14-FITC, CD16-FITC, CD19-FITC)$^{-}$, HLA-DR-PE-Cy7^{+}, CD11c-BV421^{+}, CD4-ACP-Cy7^{dim}.

Immunofluorescence of dendritic cells from peripheral blood of healthy donors

Dendritic cell subtypes were isolated from the blood of healthy donors, as described above. During the sorting time, chambered coverslip (IBIDI: cat. # 80826) were coated with 100 μL of Poly-D-Lysine 0.1 mg/ml 20′ RT and washed five times with PBS. Subsequently, 25–30.000 cells were seeded in RPMI per well and let settle for 2 h at 37°C in the incubator. After incubation, RPMI was removed, and cells were washed three times with PBS before fixation with precooled (−20°C) 1:1 acetone/methanol fixative for 30 min at −20°C. Afterward, the fixative was aspirated, and the sample was washed three times in PBS for 5 min. The cells were subsequently permeabilized in PBS with 10% normal goat serum (NGS) (Abcam, cat. # ab7481) and 0.05% Tween (PanReac AppliChem, cat. # A4974) for 10 min. After permeabilization, the cells were blocked in a blocking solution (PBS with 10% NGS +0.05% Tween 20) for >2 h at RT. Hereafter, cells were immunostained with a rabbit anti-human CECR1 (Sigma cat. # HPA007888; 1:100 in blocking solution) and anti-LAMP1-AF488 (Cell Signaling, cat. # 58996, diluted 1:200, in blocking solution) overnight at 4°C. After incubation, cells were washed three times in PBS before being incubated with goat anti-rabbit AF546 (Thermo Fisher Scientific, cat. # A-11010, 1:500) in DPBS with 10% NGS and 0.05% Tween 20 for 1h at RT. The slides were mounted with Dako mounting medium (Agilent Technologies cat. #S302380-2). The images were taken with the LSM880 (Zeiss) and analyzed with ZEN (Zeiss) and ImageJ/FiJi2.

Modeling of dsDNA binding to ADA2 and alignment of ADA2 and ADA1 structures

The crystal structure of ADA2 (3LGD, PDB DOI: https://doi.org/10.2210/pdb3lgd/pdb)[18] and double-stranded DNA (1D66) were used for protein-DNA docking using HDOCK server.[19] The top-scored complex was subjected to steered molecular dynamic simulation using a TIP3P water model in a solvated box under periodic boundary conditions. Minimization was performed using 100 steepest descent steps at 0.02 Å followed by 10 steps of conjugate gradient at 0.02 Å. Equilibration was performed for 100000 steps (time step 1fs) using the heater temperature control method. Production was performed for 100000 steps (time step 1fs). Molecular dynamic simulation was performed with UCSF Chimera. For the comparison of ADA2 and ADA1, the crystal structure of ADA2 (3LGD, PDB DOI: https://doi.org/10.2210/pdb3LGD/pdb) and ADA1 (3iar, PDB DOI: https://doi.org/10.2210/pdb3iar/pdb) were aligned with PyMOL 5.[46]

Quantification of sequence similarity between ADA2 from *Sus scrofa* and *Homo sapiens*

Amino acid sequences of ADA2 from *Sus scrofa* (P58780, https://www.uniprot.org/uniprotkb/P58780/entry) and *Homo sapiens* (Q9NZK5, https://www.uniprot.org/uniprotkb/Q9NZK5/entry) were downloaded from Uniprot and the percent of identity expressed as number of conserved amino acids on number of total amino acids.

Purification of endogenous ADA2 from porcine brain

Brains were cut into small pieces and homogenized in 0.075 M acetic acid/0.15 M NaCl (1:2 mass/vol.) using a Waring blender. The homogenate was centrifuged at 10000 g for 10 min. The supernatant was recovered, its pH adjusted by adding 1 M Tris base until the pH reached 7.6, and then heat treated at 60°C for 20 min before being again centrifuged at 10000g for 10 min. The supernatant was added to 20 mL Concanavalin A Sepharose and stirred overnight at 4°C. The slurry was run through a column and washed with PBS. The glycoproteins were eluted using 0.2 M α-methylmannoside in PBS. The protein solution was subsequently loaded onto a 20 mL hydroxyapatite column equilibrated with PBS, and the proteins were eluted at 0.05 M phosphate. After dialysis against 0.02 M Tris, pH 7.6, this fraction was applied to a DEAE anion exchange column equilibrated with the same buffer. The eluted solution was concentrated and applied to a Sephadex S-200 gel filtration column, dialyzed against 0.02 M Tris, pH 7.6, and subjected to CM cation exchange chromatography using a continuous NaCl salt gradient. The fraction eluted at 0.08 M NaCl was dialyzed against 0.02 M Tris, pH 7.6. After dialysis against 0.02 M Tris, pH 7.6, the samples were run in Heparin Sepharose chromatography, and the proteins

bound to heparin were eluted at about 0.1 M NaCl. The final eluted preparation was run on SDS/PAGE and subjected to MS/MS analyses. Mass spec data of the porcine brain ADA2 have been deposited to the ProteomeXchange Consortium via the PRIDE 48 [47] partner repository with the dataset identifier PXD019373.

Tandem mass spectrometry analysis of porcine brain proteins

Gel pieces from the heparin Sepharose solution prepared as described above were subjected to in gel reduction, alkylation, and tryptic digestion using 6 ng/μL trypsin. OMIX C18 tips (Varian, Inc., Palo Alto, CA, USA) were used for sample clean-up and concentration. Peptide mixtures containing 0.1% formic acid were loaded onto a Thermo Fisher Scientific EASY-nLC1000 system and EASY-Spray column (C18, 2 μm, 100 Å, 50 μm, 15 cm). Peptides were fractionated using a 2–100% acetonitrile gradient in 0.1% formic acid over 50 min at a 250 nL/min flow rate. The separated peptides were analyzed using a Thermo Fisher Scientific Q-Exactive mass spectrometer. Data was collected in data-dependent mode using a Top10 method. The Proteome Discoverer 1.4 software was used to generate mgf peak list files. The mgf files were searched against a mammalian database using an in-house Mascot server (Matrix Sciences, UK). Peptide mass tolerances used in the search were 10 ppm, and fragment mass tolerance was 0.02 Da.

Site-specific analysis of N-glycan structures linked to porcine brain proteins

The N-glycan analysis was carried out essentially as previously described,[48] but without spectral aligning due to the purity of the proteins. Briefly, after separation by SDS/PAGE and staining by Coomassie Blue, bands of interest were cut out and subjected to in-gel reduction, alkylation, and tryptic digestion using 6 ng/μL trypsin. OMIX C18 tips (Varian, Inc., Palo Alto, CA, USA) were used for sample cleanup and concentration. Peptide mixtures containing 0.1% formic acid were loaded onto a Thermo Fisher Scientific EASY-nLC1000 system and EASY-Spray column (C18, 2μm, 100 Å, 50μm, 15 cm). Peptides were fractionated using a 2–100% acetonitrile gradient in 0.1% formic acid over 50 min at a 250 nL/min flow rate. The separated peptides were analyzed using a Thermo Scientific Q-Exactive mass spectrometer. Data was collected in data-dependent mode using a Top10 method. The Proteome Discoverer 1.4 software was used to generate mgf peak list files. The mgf files were searched against a mammalian database using an in-house Mascot server (Matrix Sciences, UK). Peptide mass tolerances used in the search were 10 ppm, and fragment mass tolerance was 0.02 Da. The identification of the ADA2-linked glycopeptides was carried out in five steps:

1) The peptide sequences of the glycopeptides were determined by calculating the theoretical masses of the tryptic peptides containing NXS/T glycosylation sequons of the target protein. The calculated masses of these peptides attached to more than 250 different N-glycan structures were determined and compared to the peptide masses obtained from the MS/MS spectra. Those masses that matched were analyzed further. 2) The MS/MS-spectra containing glycopeptides were identified by the typical oxonium ions of simple sugars, m/z 163.1 (Hex), m/z 204.1 (HexNAc) and m/z 366.1 (HexHexNAc). Spectra containing mannose-6-phosphorylated glycans were identified by the additional ions, m/z 243.1 (PHex), and its fragmentation ion, m/z 225.1. 3) Next, each glycopeptide spectrum was scanned for fragmentation ions with a mass similar to the deglycosylated peptide and ions with an additional mass of 203.1, corresponding to linkage with a single HexNAc. 4) The identity of the peptide part was further confirmed by identifying fragmentation ions corresponding to the calculated y-and b-values. 5) The glycan structure linked to the peptide was deduced by comparing its mass from the MS/MS spectrum and theoretical masses of N-glycan structures. The glycan structures were divided into the following groups: SN3, sialylated complex structure with three GlcNAc linked to the core; SN2, sialylated complex structure with two GlcNAcs linked to the core; SN1, sialylated complex structure with one GlcNAc linked to the core; NN3, neutral complex structure with three GlcNAcs linked to the core; NN2, neutral complex structure with two GlcNAcs linked to the core; NN1, neutral complex structure with one GlcNAc linked to the core; LMF, core-fucosylated structure with 1–3 mannoses linked to the core chitobiose unit; P2M, bisphosphorylated oligomannosidic structure; P1M, monophosphorylated oligomannosidic structure; HM, oligomannose with 6–9 mannose; MM, oligomannose with 4–5 mannose; LM, oligomannose with 1–3 mannose.

Production and purification of wild-type human ADA2 and mutant ADA2 proteins

Protein production was performed in 100 mL (small scale screening), and a selection of the ADA2-mutants in 1 L (1L) (large scale) (Table S2). ADA2 open reading frame DNA (UniProt Q9NZK5: amino acids [aa] 29–511) with a CD33 leader in frame with its N terminus and a His6-tag on its C terminus (proprietary vector) was transfected with the PEI (PEI MAX, Polysciences, cat. # 24765-1) method in HKB11 mammalian cells. Freshly grown cells (1.25 x 10^8 cells) were centrifuged, resuspended in 9 mL fresh M11V3 media (produced at Bioconcept, cat. #V3-k, proprietary formulation) and transferred into 250 mL shake flask. Seventy-five μg DNA and 225 μg PEI were transferred in 1.75 mL media each and incubated for 5 min in separate tubes. After transfer of PEI to DNA and gentle mixing and incubation for another 15 min at RT, the DNA- and PEI-Mix was added to cells and incubated for 4 h in a shaking incubator (standard cultivation conditions with shaking at 115 rpm at 37°C with 5% CO2 and 80% humidity). Subsequently, transfected cells were fed with 87.5 mL M11V3-media and incubated in a shaking incubator for seven days.

Secreted His-tagged proteins from small-scale screening were purified from cell supernatant with affinity chromatography by gravity flow on the bench, with Ni-NTA-Agarose (Qiagen, cat. # 30230), with a column volume of 0.5mL. Washes have been executed with 10CV of IMAC buffer (20 mM sodium phosphate buffer, 500mM NaCl) containing 20mM Imidazol, elution has been performed with 6 CV of IMAC buffer containing 500mM Imidazol, both at pH7.4. Buffer exchange into PBS pH7.4 has been done with several concentration and dilution steps with Centrifuge Tubes Microsep Advance 10K, 516-0358, VWR. Protein integrity and purity were analyzed

by SDS-PAGE and analytical SEC on Superdex 200 Increase 10/300 GL column, GE28-9909-44, with PBS, pH7.4 as running buffer, on Agilent 1260 Infinity instrument.

The transfection protocol was scaled up proportionally for a 1L large-scale expression of a selection of ADA2-variants. These supernatants were purified on an Äkta system (GE Healthcare), with a 5mL HisTrap HP prepacked column with Nickel Sepharose (17-5248-02, GE Healthcare), using the same buffers as described for small scale but with gradient elution. Polishing of these proteins on preparative SEC was done on a Superdex75 column, GE Healthcare, 28-9893-33, with PBS pH7.4.

Protein integrity and purity were analyzed by SDS-PAGE, analytical SEC on a Superdex 200 Increase 10/300 GL column, GE28-9909-44, with PBS, pH7.4 as running buffer, on an Agilent 1260 Infinity instrument, and MS analysis. All proteins showed low aggregation and an identical retention time.

For wild-type ADA2 and the ADA2 G47A mutant, inline multi-angle light scattering (MALS) was combined with SEC to confirm the molecular weight of 127kDa of the recombinant protein resembling the mass of an ADA2 dimer. In brief, a Superdex 200 10/30 GL column (GE HealthCare) was equilibrated with PBS (Sigma D8537), and samples were run on an Agilent 1200 HPLC system coupled with Wyatt MALS instrumentation at a constant 0.5 mL/min flow. Human Macrophage colony stimulating Factor1-Receptor (aa 20–512), which comprises nearly the complete extracellular domain of hCSF1-Receptor (aa 20–517; UniprotKB-P07333, full-length aa 1–972) and a His-tag, was expressed and purified as ADA2 using an IMAC column and used as a control.

Hereafter is reported a brief summary of the ADA2 mutant proteins described in patients with ADA-deficiency and tested in the manuscript. In brackets is reported the paper where the variant has been originally described.

E328K (Keer et al,[49] 2016): The variant is localized in the catalytic domain. ADA2 activity in the patient's plasma, measured using HPLC [2] was 1.7 mU/ml, significantly below the level in healthy controls [mean (s.d.) 14 (6.1) mU/ml]. A variant affecting the same amino acid (E328D) has been tested functionally in Lee et al,[50]2020 and has shown no residual ADA activity.

G358R (Hashem et al,[51] 2017): The variant is localized in the catalytic domain. Reported in two different patients who underwent HSCT in the original paper. The variant has also been tested functionally in Lee et al,[50]2020 and has shown no residual ADA activity.

G47R (Zhou et al,[11] 2014): The variant is localized in the dimerization domain. This is a frequent variant reported in several papers and individuals. The variant has also been tested functionally in Lee et al,[50]2020 and has been shown to have less than 25% of residual ADA activity.

P344L (Caorsi et al,[52] 2017): The variant is localized in the catalytic domain. Reported originally in Caorsi et al,[52] 2017 in compound heterozygosity (C.H) in two patients with different clinical phenotypes. The variant has also been tested functionally in Lee et al,[50]2020 and has been shown to have approximately 50% of residual ADA activity.

P193L (Belot et al,[53] 2014): The variant is localized in the catalytic domain. It was reported in a patient in C.H. with the Arg169Gln in a patient with an upregulation of interferon-stimulated gene transcripts in peripheral blood. To our knowledge, the variant has been tested functionally only in our manuscript.

Mass spectrometric analysis of recombinant human ADA2

1 μg of protein was resuspended in 8M urea, 10 mM HEPES (pH 8), and 10 mM DTT. Alkylation was performed in the dark for 30 min by adding 55 mM iodoacetamide (IAA). A two-step proteolytic digestion was performed. First, samples were digested at room temperature (RT) with LysC (1:50, w/w) for 3h. Then, they were diluted 1:5 with 50 mM ammonium bicarbonate (pH 8) and digested with trypsin (1:50, w/w) at RT overnight. The resulting peptide mixtures were acidified and loaded on C18 StageTips. Peptides were eluted with 80% acetonitrile (ACN), dried using a SpeedVac centrifuge (Savant, Concentrator plus, SC 110 A), and resuspended in 2% ACN, 0.1% trifluoroacetic acid (TFA), and 0.5% acetic acid. Peptides were separated on an EASY-nLC 1200 HPLC system (Thermo Fisher Scientific) coupled online to a Q Exactive mass HF spectrometer via a nanoelectrospray source (Thermo Fisher Scientific). Peptides were loaded in buffer A (0.1% formic acid) on in-house packed columns (75 μm inner diameter, 50 cm length, and 1.9 μm C18 particles from Dr. Maisch, GmbH). Peptides were eluted with a non-linear 120 min gradient of 5%–60% buffer B (80% ACN, 0.1% formic acid) at a 250 nL/min flow rate and a column temperature of 50°C. Raw files were analyzed by MaxQuant software (version 1.5.3.54). The mass spectrometry proteomics data have been deposited to the ProteomeXchange Consortium via the PRIDE[47] partner repository with the dataset identifier PXD019382.

FRET assay of wt and mutant human recombinant ADA2

ADA2 FRET assay of recombinant human ADA2 was measured by a commercial FRET assay (DNaseAlert, Thermo Fisher Scientific, cat. # AM1970). In brief, 6 μL ADA2 solution at a final concentration of 10 μg/mL was incubated with 3 μL DNA substrate and 40 μL of MIB super buffer 2 (Malonic acid: imidazole: boric acid in the molar ratios 2:3:3) or CHC super buffer 1 (Citric acid: HEPES: CHES in the molar ratios 2:3:4) (Jena Bioscience CS-332- JBScreen Thermofluor Fundament) at the indicated pH and NaCl concentration. ADA2-DNA interaction was measured every 2 min for 30 min with a fluorescent reader (Spectramax, excitation 535 nm and emission 575 nm). FRET activity was measured at 25 μg/mL.

ADA activity of wt and mutant human recombinant ADA2 proteins

Adenosine Deaminase (ADA) activity was measured by a commercial assay (Diazyme-DZ117A-K), which is specific for ADA and has no detectable reaction with other nucleosides. 5 μL of ADA2 or control proteins were added to 180 μL of buffer R1 and incubated for 3 min at 37°C, then 90 μL of buffer R2 was added and the plate was incubated at 37°C for 20 min. The enzymatic activity was

monitored by measuring the OD at 550 nm with a temperature-controlled fluorescent reader (Synergy H1 from Biotek). The kit was calibrated with the internal ADA calibrator, which was in the kit specification's expected range. A range of concentrations was measured to describe the activity of the ADA2 recombinant proteins, and the EC50 value was calculated using Prism Software (GraphPad).

Electrophoretic mobility shift assay (EMSA)

Oligonucleotide substrates (Table S1) were 5′-end labeled using T4 polynucleotide kinase (New England Biolabs, cat. #M0201) and [γ-32P]ATP (3000 Ci/mmol, Amersham Biosciences). Double-stranded (ds) substrates were generated by annealing (65°C, 3 min) the labeled single-stranded (ss) oligonucleotide to a complementary strand. All substrates were gel-purified before use. In EMSA, ADA2 (wt or ADA2 mutant proteins; 0.2–1.5 pmol) and labeled substrates (10 fmol) were mixed in 25 mM sodium acetate (NaAc) pH 5.5 in 10 μL reaction volume. Samples were incubated on ice for 15 min, and DNA gel loading dye (6x) was added (Thermo Fisher Scientific cat. #R0611). DNA-ADA2 complexes were separated from unbound substrates on 7% native polyacrylamide gels containing 2% glycerol in 0.5x TBE at 120 V for 45 min on ice. Gels were dried and visualized by phosphorimaging (Amersham Typhoon IP), and ImageQuant IQTL 8.2 was used for quantification (Cytiva). For the test of pH dependence, the buffer was 25 mM Tris-HCl pH 7.5.

DNA deaminase assay

DNA deaminase activity was measured using the labeled DNA substrates and amounts of recombinant ADA2 (WT or mutants) as indicated in 25 mM NaAc pH 5.5 in 10 μL reaction volume. Incubation was at 37°C for 40 min or as shown in the figures, and reactions were neutralized by adding 2 μL 0.1M Tris-HCl pH 9.3. Deoxyinosines were detected using in-house purified *Escherichia coli* (Ec) EndoV. The EcEndoV open reading frame was cloned in pET28b (Novagen, cat. # 69865) in a frame with a c-terminal His-tag, and the protein was purified by Ni-NTA affinity chromatography after expression in the *E. coli* strain ER2566 (New England Biolabs, cat. #C2566). EcEdnoV (0.8 pmol) and 2.5 μL EcEndoV reaction buffer (final 10 mM Tris-HCl pH 8.5, 2 mM MgCl2, 50 mM KCl, 1 mM DTT, 5% glycerol) were added to the reaction and incubated at 37°C for 15 min. Samples were added formamide loading dye (95% formamide, 5 mM EDTA, 0.05% bromphenol blue, and 0.05% xylene cyanol), denatured at 60°C for 3 min, and the reaction products separated on 20% polyacrylamide/urea gels at 200 V for 1 h in 1× taurine buffer. All experiments were performed at least 2–3 times, and representative experiments are shown. The influence of pH on ADA2-mediated dT-to-dI activity was tested in NaAc buffer (pH 4.0–6.5) or Tris-HCl (pH 7.0). Gels were dried and visualized by phosphorimaging (Amersham Typhoon IP), and ImageQuant IQTL 8.2 was used for quantification (Cytiva).

DNA dot blot

Human recombinant ADA2 (25–100 fmol) was incubated with substrates (10 pmol) as indicated for 1 h in 25 mM sodium acetate pH 5.5 at 37°C in 5 μL reactions. Reactions were neutralized with 0.5 μL 100 mM Tris-HCl pH 9.3 and heat denatured at 60°C for 3 min 2.5 μL of the reaction was spotted onto a nitrocellulose membrane (Whatman Protran BA83) that was air dried before crosslinking (120 mJ/cm^2) the DNA to the membrane. Inosines in DNA were detected using an anti-inosine antibody (Medical and Biological Laboratories; cat. # PM098, dilution 1:1000 in PBS with 5% nonfat dry milk), HRP-conjugated secondary antibody (Goat anti-rabbit IgG, Vector laboratories cat. #P1-1000-1) and Supersignal West Femto Maximum Sensitivity Substrate (Thermo Fisher Scientific cat. # 34094). As a control of the specificity of the antibody, oligonucleotides with and without inosines were tested in dot blot. Despite being raised against inosines in RNA, the antibody recognized inosines in DNA oligonucleotides (ACTGGACAIITICTCCGAGG and CCTCGGAGTITTTGTCCAGT), whereas a DNA oligonucleotide without inosine (GCTGGACAAATACTCCGAGG) gave no signal.

Nucleobases content in DNA by mass spectrometry

Oligonucleotides (150 fmol) were incubated with human recombinant ADA2 (hrADA2) (100 fmol) in 25 mM ammonium acetate (pH 5.5) in 20 μL reaction volume for 45 min. Samples were heated at 80°C for 5 min before completely dried under vacuum. The samples' deoxyinosine (dI) content was measured by liquid chromatography-mass spectrometry (LC-MS/MS). DNA was dissolved in 100 μM deaminase inhibitor EHNA (Sigma-Aldrich cat. #E114) and hydrolyzed to nucleosides by 20 U benzonase (Santa Cruz Biotech cat. # sc-391121B), 0.2 U nuclease P1 (Sigma-Aldrich cat. #N8630), and 0.1 U alkaline phosphatase (Sigma-Aldrich cat. #P5931) in 10 mM ammonium acetate pH 6.0, and 1 mM $MgCl_2$ at 40°C for 40 min, added 3 volumes of acetonitrile and centrifuged (16 000g, 30 min, 4°C). The supernatants were lyophilized at −80°C to minimize spontaneous adenine deamination during drying and dissolved in 50 μL water for LC-MS/MS analyses of dI, inosine, and unmodified nucleosides. Chromatographic separation was performed using an Agilent 1290 Infinity II UHPLC system with a ZORBAX RRHD Eclipse Plus C18 150 × 2.1 mm ID (1.8 μm) column protected with a ZORBAX RRHD Eclipse Plus C18 5 × 2.1 mm ID (1.8 μm) guard column (Agilent). For dI and inosine analyses, the mobile phase consisted of water and methanol (both added 10 mM acetic acid) run at 0.25 mL/min, starting with 5% methanol for 0.5 min, followed by a 4 min gradient of 5–90% methanol, and 4 min re-equilibration with 5% methanol. A portion of each sample was diluted to analyze unmodified nucleosides, chromatographed isocratically with water/methanol/formic acid (80/20/0.1%). Mass spectrometric detection was performed using an Agilent 6495 Triple Quadrupole system with electrospray ionization, for DNA monitoring the mass transitions 251.1/135.1 (dI, negative mode), 252.1/136.1 (dA, positive mode), 228.1/112.1 (dC, positive mode), 268.1/152.1 (dG, positive mode) and 243.1/127.1 (dT, positive mode), and for RNA monitoring 267.1/135.1 (I, negative mode), 268.1/136.1 (A, positive mode), 244.1/112.1 (C, positive mode), 284.1/152.1 (G, positive mode) and 245.1/113.1 (U, positive mode).

DNA sequencing gel

Sequencing gels were the same 20% polyacrylamide/urea/taurine gels as the ones described in the deamination assay section, but they were run at 35 W for 1 h. The gels were dried, and radiolabeled fragments were visualized as above.

DNA deaminase competition assay

In the competition assays, competitors and ADA2 were preincubated on ice for 5 min in 25 mM NaAc pH 5.5 before the labeled DNA substrate was added, as described in the deamination assay section. Incubation continued at 37°C for 30 min before neutralization and treatment with EcEndoV as above. The following competitors were used: adenosine, deoxyadenosine, A-DNA (oligo IITI | 24522 of Table S1), non-A-DNA (oligo | 24793 of Table S1), deoxycoformycin (Sigma-Aldrich, cat. # 116860). All experiments were performed at least 2–3 times, and representative experiments are shown.

RNA deaminase assay

Oligonucleotide substrates (Table S1) were 5′-end labeled using T4 polynucleotide kinase (New England Biolabs, cat. #M0201) and [γ-32P]ATP (3000 Ci/mmol, Amersham Biosciences). Subsequently, RNA deaminase activity was measured using the labeled RNA substrates and amounts of recombinant ADA2 (wt or mutants) as indicated in 25 mM NaAc pH 5.5 in 10 μL reaction volume. Incubation was at 37°C for 40 min or as shown in the figures, and reactions were neutralized by adding 2 μL 0.1M Tris-HCl pH 9.3. Detection of inosines was done using in-house purified human EndoV. Protein was expressed and purified as described in Vik E.S. et al. Nat Commun 2271 (2013). hEndoV (0.8 pmol) and 2.5 μL EndoV reaction buffer (final 10 mM Tris-HCl pH 8.5, 2 mM MgCl2, 50 mM KCl, 1 mM DTT, 5% glycerol) were added to the reaction and incubated at 37°C for 15 min. Samples were added formamide loading dye (95% formamide, 5 mM EDTA, 0.05% bromphenol blue, and 0.05% xylene cyanol), denatured at 60°C for 3 min, and the reaction products separated on 20% polyacrylamide/urea gels at 200 V for 1 h in 1× taurine buffer.

TLR9 activation via HEK TLR9-SEAP reporter cells

Human TLR9 reporter HEK 293 Cells (NF-kB), cat. # hkb-htlr9 were cultured as described above and stimulated according to the recommendations of the manufacturer's protocol. Briefly, cells were detached and resuspended in warm PBS, counted, resuspended (80.000 cells/180 μL of HEK-Blue Detection medium) and mixed with 20 μL of different stimuli (Oligos) at different concentrations as indicated in the respective figures and incubated overnight. TLR9 activation was measured with HEK-Blue Detection cell culture medium. Secreted embryonic alkaline phosphatase (SEAP) activity was determined by measuring optical density (OD) at 620–655 nm.

ADA2 expression and TLR7 and TLR9 activation via HEK 7/9-UNCB93B1 reporter cells

The 293XL/hTLR7-HA and 293XL/hTLR9-HA cell lines (Invivogen) both expressing human UNC93B1-mCitrine[27] +1WT were plated at 20.000 cells/100μL in a 96-well plate. Once adherent, they were transiently transfected with 25ng pLenti-IRES-GFP-Puro or pLenti-ADA2-IRES-GFP-Puro as indicated using Mirus-LT1 according to the manufacturer's instructions. 20h after plasmid transfection, cells were stimulated with 1 μg/mL R848 or 10μg/mL of E.coli DNA, CpG2006, CpG2216 or 9.2sRNA complexed with 5μL DOTAP for 10 min. After 16h, cellular supernatants were harvested for ELISA. The day of stimulation cells were detached and resuspended in warm PBS, counted, resuspended (80.000 cells/180 μL of HEK-Blue Detection medium) and mixed with 20 μL of different stimuli at different concentrations (Oligos) as indicated in the respective figures and incubated overnight. TLR9 activation was measured by quantifying IL8 production by ELISA.

Lentivirus transduction of HEK-Blue hTLR9 reporter cells with ADA2 or empty vector

Lentivirus were produced by transfecting HEK293 T cells with psPAX2, pMD2.G and pLenti-ADA2-IRES-GFP-Puro or pLenti-ADA2-IRES-GFP-ADA2-Puro (Amount per 10 cm dish, respectively 1.3 pmol, 0.72 pmol, 1.64 pmol). Plasmids were transfected by diluting the plasmids in 1 mL Opti-MEM containing a ratio of 1:3 between DNA and PEI (1 mg/ml). The transfection mix was added to HEK293T packaging cells and incubated 18hrs. After incubation the medium was removed and replaced with 15 mL of fresh medium. Supernatants containing virus was harvested at 48 and 72 h, centrifuged at 500 g for 5 min and filtered through 0.45 μm filter. Subsequently, the supernatants were transferred to HEK Blue hTLR9 reporter cells and incubated for 16 h in a humidified incubator in an atmosphere of 5–7% CO2. After this time, the media containing lentiviral particles was removed and substituted with fresh medium. The efficiency of transduction was monitored by measuring GFP expression using flow cytometry. GFP-positive cells were FACS sorted, and the expression of ADA2 was evaluated by Western Blot.

Measurement of type-I IFN production with IFN-α/β reporter HEK 293 cells from PBMCs

The day of measurement, HEK-Blue IFN-α/β cells were detached, diluted to a concentration of 280.000 cells/ml, and subsequently seeded in a flat-bottomed 96-well plate at 50.000 cells/well density. To generate a standard curve, a series of 10-fold dilutions of recombinant human IFN-α was prepared with an initial concentration of 2 μg/mL. The cells were then incubated for 24 h with either 20 μL of the supernatant of the stimulated cells or with the recombinant human IFN-α overnight at 37°C. Each experimental condition was carried out in triplicate. After incubation, the QUANTI-Blue solution was prepared according to the manufacturer's instructions, and 20 μL of the supernatants from the HEK-Blue IFN-α/β mixed with 180 μL of the QUANTI-Blue solution and incubated for

30–40 min at 37°C. The levels of SEAP, which served as an indicator of IFN production, were measured by spectrophotometry at a wavelength of 620 nm.

Measurment of type-I IFN production in PBMCs

PBMCs were isolated from healthy donors and resuspended in RPMI medium supplemented with 10% FBS and 100U/ml P/S and subsequently seeded into round-bottomed 96-well plates (90.000 cells/well in a final volume of 100 μL). Cells were stimulated overnight with CpG (final concentration 3 μg/mL) or CpI (final concentration 3 μg/mL) or CpA (final concentration 3 μg/mL) or CpC (final concentration 3 μg/mL) or PolyIC (final concentration 1 μg/mL). After stimulation 20 μL of the supernatants were used to measure type-I IFN production with IFN-α/β reporter HEK 293.

Immune stimulation of PBMCs

Blood was obtained from DADA2 patients or age and sex-matched healthy donors in EDTA tubes. PBMCs were prepared by centrifugation on a Pancoll gradient (PAN Biotech, Pancoll human cat. #P04-60500). Cells were seeded in 96 well round bottom plate (10^6 cells/well) in 200 μL of RPMI containing 10% heat inactivated fetal bovine serum, 100 U/ml penicillin, 100 μg/mL streptomycin and stimulated overnight with CpG2216 (10 μg/mL), or CpG2006 (10 μg/mL), or 9.2sRNA (2 μg/mL). Supernatants were harvested after 16h of stimulation for the quantification of TNF or IFN-α by ELISA.

Measurement of type-I IFN production in dendritic cells (DCs)

Blood was obtained from DADA2 patients or age and sex-matched healthy donors in EDTA tubes. PBMCs were prepared by centrifugation on a Pancoll gradient (PAN Biotech, Pancoll human cat. #P04-60500). Plasmacytoid dendritic cells (pDCs) were sorted as viability-dy BV 510^-, lineage (CD3-FITC, CD14-FITC, CD16-FITC, CD19-FITC)$^-$, HLA-DR-APC$^+$, CD11c-BV421^{dim}, CD4-PE^{high}, conventional DC (cDCs) as lineage (CD3-FITC, CD14-FITC, CD16-FITC, CD19-FITC)-, HLA-DR-APC$^+$, CD11c-BV421$^+$, CD4-PE^{dim}. Cells were seeded in 96 well V bottom plate (500 cells/well) and stimulated overnight with CpG 2216 (5 μM). The day after 20 μL of the supernatant of the stimulated DCs the supernatants were used to measure type-I IFN production with IFN-α/β reporter HEK 293.

Measurement of type-I IFN production in PBMCs Is upon stimulation with PLA conjugated DNA

Blood was obtained from DADA2 patients or age and sex-matched healthy donors in EDTA tubes, and PBMCs were prepared by centrifugation on a Pancoll gradient (PAN Biotech, Pancoll human cat. #P04-60500). Cells were seeded in 96 well V bottom plates (90.000 cells/well in a final volume of 100μL). Oligo 259 and 260 (Table S1) were annealed and complexed with PLA (Sigma cat #P 4663) at a ratio of 1μg DNA/1.2 μL PLA in PBS (0.4 μg dsDNA, 0.6μL PLA and 30μL of PBS for each well) and incubated 30 min at RT. After incubation, the DNA was added to the cells and incubated at 37°C for 17 h. The day after the production of type-I IFN was measured using HEK-Blue IFN-α/β reporter cells as described above.

QUANTIFICATION AND STATISTICAL ANALYSIS

Statistical analyses were performed with GraphPad Prism 8. The tests performed for statistical analyses are indicated in the respective figure legends.